

Out-of-distribution generalisation for learning quantum channels with low-energy coherent states

Jason L. Pereira,^{1,2,3,*} Quntao Zhuang,^{2,4} and Leonardo Banchi^{5,1}

¹*INFN Sezione di Firenze, via G. Sansone 1, Sesto Fiorentino (FI) I-50019, Italy*

²*Ming Hsieh Department of Electrical and Computer Engineering,*

University of Southern California, Los Angeles, California 90089, USA

³*Sorbonne Université, CNRS, LIP6, 4 Place Jussieu, Paris F-75005, France*

⁴*Department of Physics and Astronomy, University of Southern California, Los Angeles, California 90089, USA*

⁵*Department of Physics and Astronomy, University of Florence,*

via G. Sansone 1, Sesto Fiorentino (FI) I-50019, Italy

(Dated: February 10, 2025)

When experimentally learning the action of a continuous variable quantum process by probing it with inputs, there will often be some restriction on the input states used. One experimentally simple way to probe the channel is using low-energy coherent states. Learning a quantum channel in this way presents difficulties, due to the fact that two channels may act similarly on low energy inputs but very differently for high energy inputs. They may also act similarly on coherent state inputs but differently on non-classical inputs. Extrapolating the behaviour of a channel for more general input states from its action on the far more limited set of low energy coherent states is a case of out-of-distribution generalisation. To be sure that such generalisation gives meaningful results, one needs to relate error bounds for the training set to bounds that are valid for all inputs. We show that for any pair of channels that act sufficiently similarly on low energy coherent state inputs, one can bound how different the input-output relations are for any (high energy or highly non-classical) input. This proves out-of-distribution generalisation is always possible for learning quantum channels using low energy coherent states.

I. INTRODUCTION

Many physical systems can be modelled as quantum channels, which map one (input) quantum state into another (the output). Learning about a physical process can therefore be regarded as the task of finding the input-output relations of the enacted quantum channel [1]. Experimentally, we would do this by sending probe states through the channel and characterising the outputs. However, a full characterisation can be very “expensive” in terms of the number of experiments required. This is especially true for continuous variable (CV) systems [2, 3]. Since the dimension is infinite, it is not possible to, for example, probe a channel with every basis state individually.

Instead, we must probe the channel with some finite set of input states and then extrapolate the results to all possible inputs. One particularly simple set of input states is the coherent states. These are classical states that can easily be generated experimentally. However, they form an overcomplete basis, so are sufficient to characterise a CV channel [4–7]. In any real experiment, we will also have a maximum energy for our probe states, so the inputs will be restricted to coherent states of bounded energy.

Whenever we extrapolate from limited data, we need to understand how reliable our learned answer is outside of our limited dataset, i.e., whether it generalises. The problem is compounded if we want our solution to hold even outside of the parameter region in which our dataset lies. If our dataset consists of only the outputs for low energy, classical inputs, we may wonder how reliable our input-output relations are for higher energy or non-classical systems. This is called out-of-distribution generalisation.

The problem of out-of-distribution generalisation for learning quantum channels has been investigated in the discrete variable, unitary case [8, 9]. In [8], it is shown that by probing a unitary with a restricted set of input states, one can learn how it acts on a very different set of inputs. In the CV case, it is known that we can extrapolate the input-output relations for coherent states to general states [4, 5], but not how an uncertainty in those relations for coherent states propagates when applied out-of-distribution to general states. Since we will never learn the action of a process perfectly (with finite samples), even on a limited set of inputs, an understanding of out-of-distribution error propagation is crucial.

CV channels are particularly important, as they model various quantum sensing and communication systems, such as optomechanical systems [10–12], microwave cavity quantum electrodynamics (cQED) systems [13], radiofrequency-photon sensors [14], radar and lidar detection [15], optical spectroscopy processes [16–19], optical communication and quantum networks [20, 21], nanophotonic chips for machine learning [22], and optical quantum computers [23].

In this work, we present a general formalism for understanding out-of-distribution generalisation in CV channels. We show that if any pair of CV channels has sufficiently close outputs for low energy coherent state inputs, it is possible to construct a

*Electronic address: Jason.Pereira@lip6.fr

bound on the output distance for any input state. Hence, we prove that out-of-distribution generalisation is always possible for learning quantum channels using low energy coherent states.

We start, in Section II, by introducing the problem and giving an overview of our main results. In Section III, we go into more detail about the generalisation from low energy coherent states to higher energy coherent states. In Section VI, we investigate some examples of this type of generalisation. In Section IV, we show the extension from coherent states to general states, and in Section VII, we give examples of this extension. In Section VIII, we present our conclusions.

II. OVERVIEW

Learning a quantum channel means understanding how any input state will be mapped to an output state by that channel. We can express our knowledge of the target channel as a “learned” channel that mimics as closely as possible the input-output relations of the target. This knowledge could (non-exhaustively) take the form of a classical description of the input-output relations, the parameter values for a specific form of parametrised channel, or some set of settings for a physical device that lets us enact the learned channel. The better we learn the target channel, the closer the two channels will be.

Our aim is to bound the error in learning the action of a CV channel on an arbitrary state after learning on samples from a restricted set of input coherent states. Specifically, we want to bound the distance (trace norm) between the output of a target channel, Ψ , and our learned channel, Φ , for test state ρ , with average photon number \bar{n} . To be useful (non-trivial), the bound on $\|\Psi[\rho] - \Phi[\rho]\|$ should approach 0 as we learn Ψ better over our restricted set of inputs.

If such a bound exists, this tells us that *out-of-distribution generalisation is possible*, in the sense that learning the input-output relations for a very restricted set of classical state inputs is sufficient to mimic them for completely general (including highly non-classical) input states. The tightness of the bound depends on the class of channels to which Ψ and Φ belong, e.g. Gaussian [3, 24], unitary operation, etc. If ρ has a known, finite negativity (of its P-representation) \mathcal{N} [25], we may also wish to take this into account to obtain a tighter bound. A bound of this type can be constructed in three stages (as illustrated in Fig. 1).

1. Given N samples of low energy coherent states sent through a channel Ψ , bound the error in learning the action of this channel on the same distribution of low energy coherent states. Specifically, we have N samples of the form $\Psi[|re^{i\phi}\rangle\langle re^{i\phi}|_{\text{coh}}]$, for $r \leq \tau$. Find a protocol that uses them to learn a channel Φ , such that (with high probability) $\|(\Psi - \Phi)[|re^{i\phi}\rangle\langle re^{i\phi}|_{\text{coh}}]\| \leq \epsilon_0$ for all $r \leq \tau$, where ϵ_0 is a decreasing function of N (so that more samples let us learn the channel better). I.e., we bound the “in-distribution” error for learning the action of channel Ψ on coherent states with an average photon number of $\leq \tau^2$. Decreasing ϵ_0 means using more samples to find a new channel Φ , such that the output distance (for our subset of coherent states) is smaller. We require that $\epsilon_0 \rightarrow 0$ as $N \rightarrow \infty$.
2. Assume stage 1 was successful. Find a function $\epsilon(\epsilon_0, r^2)$ such that $\|(\Psi - \Phi)[|re^{i\phi}\rangle\langle re^{i\phi}|_{\text{coh}}]\| \leq \epsilon(\epsilon_0, r^2)$ for all r . This is a restricted case of out-of-distribution generalisation. We also require that $\epsilon(\epsilon_0, r^2)$ is a decreasing function of ϵ_0 that reaches 0 for $\epsilon_0 = 0$, ensuring that our out-of-distribution error reaches 0 if our in-distribution error does.
3. Assume stage 2 was successful. For an arbitrary input ρ , bound $\|(\Psi - \Phi)[\rho]\|$ in terms of $\bar{n}(\rho)$, $\epsilon(\epsilon_0, r)$, and possibly $\mathcal{N}(\rho)$ (if finite). This gives us a complete bound for out-of-distribution generalisation in the general case, and we require that it reaches 0 for $\epsilon = 0$.

The first stage involves using a limited set of inputs to probe a quantum process and applying in-distribution generalisation to bound the error over this set. Learning the input-output relations for a channel over a limited set of states is a somewhat underspecified problem, since any concrete statements about it would strongly depend on the learning process and the classes of channel under consideration. This is intentional, since the aim of this paper is to be as general as possible and to give a formalism for extending a bound for low energy coherent state inputs to general states, regardless of how the initial bound was obtained. However, in Section V, we discuss briefly how this task has been addressed in the frameworks of quantum process tomography, quantum metrology and quantum machine learning. Elsewhere, we do not focus on this step, but rather assume we already have the bound $\|(\Psi - \Phi)[|re^{i\phi}\rangle\langle re^{i\phi}|_{\text{coh}}]\| \leq \epsilon_0$ (for $r \leq \tau$) and want to extend it to more general inputs.

We focus on the remaining two stages. Our goals are twofold: we want to make some general statements that hold for all classes of channels and all input states and we also want to give tighter bounds for cases in which we have more information about the channels and/or input states. Our main results can be informally summarised as follows:

1. If two channels have exactly the same output for low energy coherent state inputs, they also have the same output for high energy coherent state inputs.
2. If two channels have sufficiently similar outputs (i.e., a tightly bounded output distance) for low energy coherent state inputs, they also have a bounded output distance for high energy coherent state inputs. As the channel outputs become more similar for low energy inputs, they also become more similar for high energy inputs (as one bound converges to 0, the other does too). For particular example classes of channels, we derive explicit bounds.

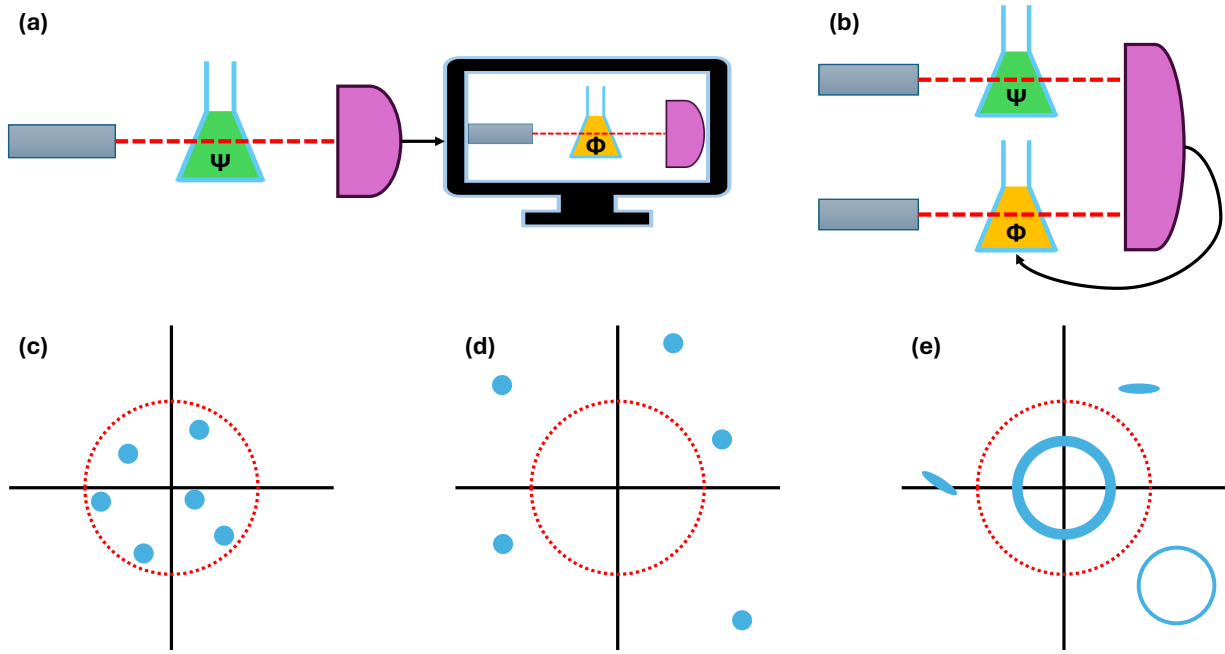


FIG. 1: Parts (a) and (b) show two different ways we could learn a channel, Φ , that mimics the action of a target process, Ψ , for low energy coherent states. (a) is “classical” learning of a quantum channel, whilst (b) is a form of quantum machine learning. In this illustration, we depict probing the optical properties of an unknown (green) sample, although the process could be a magnetic field, a non-linear medium, a reflective cavity, or any other transformation that could be applied to a state of light. We search through a set of possible (yellow) optical mediums to find the one that best imitates the green substance. In (a), we use a (finite energy) laser to send low energy coherent states through the target and characterise the outputs with measurements. The results are post-processed (e.g., by feeding them into a classical computer, per the diagram) to obtain classical knowledge of the input-output relations. We can then “simulate” the action of Ψ on an unknown state, using our classical computer and the transformation Φ . In (b), we have a tuneable quantum device (such as a different substance with tuneable optical properties, a tuneable magnetic field, or some parametrised optical circuit) that we want to use to imitate the target process. We probe both processes with the same coherent states (we show two lasers, but a real implementation could use a single laser and a balanced beamsplitter, to ensure the probing states are identical). Instead of characterising both outputs, we measure them jointly, to determine their trace distance. We could then use the measurement results to tune the quantum device and so reduce the distance. Once Φ is tuned, we hope that an unknown state sent through the quantum device will be transformed similarly to if it were sent through Ψ . Parts (c-e) illustrate the three types of input for which we can bound the closeness of two channels. (c) corresponds to the input states for parts (a) and (b); the probes used in our physical measurements are low energy coherent states. The dotted line shows the maximum average energy of the inputs. We can construct a bound on the output distance between our target and learned processes, Ψ and Φ , based on our measurement results. In (d), we consider higher energy coherent state inputs. These are outside of the class of inputs for which we have actual measurement results; rather, we want to be able to trust that our simulation, Φ , of Ψ is still accurate for these inputs (in the scenario of part (a)) or that our tuned quantum device still mimics our target well (in the scenario of part (b)). We use our bound for the inputs shown in (c) to construct a bound on the inputs shown in (d). The scaling of this bound depends on the class of channels to which the target and learned channel belong. In (e), we consider other types of input states, including non-classical states such as squeezed vacuums and Fock states. We again want to trust that Φ is a good simulation of Ψ for these types of input, and so we extend our bounds for the inputs in (d) to the inputs in (e).

3. If two channels have similar outputs for coherent state inputs, they also have a bounded output distance for any input state. As the channel outputs become more similar for coherent states, they also become more similar for general inputs. We give explicit expressions for particular examples of non-classical states.

Together, these results show that *out-of-distribution generalisation is possible for every input state and all target channels*.

A. Main results: Out of distribution generalisation for coherent states

We start by investigating how the output distance between a pair of channels, for a coherent state input, scales with the energy of the input. The question we want to answer is: *if the outputs of two channels are close for low energy coherent state inputs, how quickly do they become far apart as the input energy increases?* The first observation we make (proven in Appendix B) is:

Theorem 1 Suppose $\|(\Psi - \Phi)[|re^{i\phi}\rangle\langle re^{i\phi}|_{\text{coh}}]\| = 0$ for all ϕ and all $r \leq \tau$, for some $\tau > 0$. Then, for all ϕ and all r , $\|(\Psi - \Phi)[|re^{i\phi}\rangle\langle re^{i\phi}|_{\text{coh}}]\| = 0$.

In other words, if we learn the action of a channel exactly on an (infinite but compact) subset of the coherent states, we also learn it exactly on all coherent states. Whilst intuitive, this is important to state, as otherwise one might think there are pairs of channels that exactly coincide for low energy coherent states but that diverge elsewhere in phase space. This follows from the overcompleteness of the coherent states, or alternatively from the fact that every differential of every matrix element (in any basis) of $(\Psi - \Phi)[|re^{i\phi}\rangle\langle re^{i\phi}|_{\text{coh}}]$ is identically zero, and is in line with what we might expect from [5].

On the other hand, even if we can only bound the error on the subset with some $\epsilon_0 > 0$, we can still bound the error for all coherent states. In Appendix I, we show:

Theorem 2 *Suppose $\|(\Psi - \Phi)[|re^{i\phi}\rangle\langle re^{i\phi}|_{\text{coh}}]\| \leq \epsilon_0$ for all ϕ and all $r \leq \tau$, for some $\tau > 0$. Then, there exists a concave (in r^2) function $\epsilon(\epsilon_0, r^2)$ such that $\|(\Psi - \Phi)[|re^{i\phi}\rangle\langle re^{i\phi}|_{\text{coh}}]\| \leq \epsilon(\epsilon_0, r^2)$ for all ϕ and r , with the following properties:*

1. For any r and for $\epsilon'_0 < \epsilon_0$, $\epsilon(\epsilon'_0, r^2) \leq \epsilon(\epsilon_0, r^2)$.
2. For any r , $\epsilon(\epsilon_0, r^2) \rightarrow 0$ as $\epsilon_0 \rightarrow 0$.

We express ϵ as a function of r^2 , rather than r , since r^2 is the mean photon number and so is a more natural variable to use. This theorem shows that if we learn a channel sufficiently well on a subset of the coherent states, our target and learned channel will also have similar outputs for coherent states outside of that subset.

Although Theorem 2 shows the existence of a bounding function $\epsilon(\epsilon_0, r^2)$ that is non-trivial for sufficiently small ϵ_0 (and, in fact, the proof is constructive), the function found in Appendix I requires very small ϵ_0 to be non-trivial for large r . It is therefore better to find channel-specific ϵ -functions. In Section VI, we use specific examples to demonstrate how we can obtain analytical expressions for the function $\epsilon(\epsilon_0, r^2)$ in certain cases, e.g., if our target channel is in a known class.

B. Main results: Out of distribution generalisation for general states

Next, we address more general states. The question now is: *if the outputs of two channels are within a bounded distance of each other for coherent state inputs, how far apart are they for other types of input states?* We now assume we have a function $\epsilon(\epsilon_0, r^2)$ that upper bounds the trace norm between channel outputs for a coherent state input. Starting from this function, the goal is to prove a bound on the trace norm between channel outputs for any bounded energy input state ρ .

Such a bound can be obtained using the P-representation of CV states and the convexity of the trace norm. The calculations are outlined in Section IV and presented in greater detail in the Appendices. In the most general case, the output distance for any non-classical input can be bounded with the following theorem:

Theorem 3 *Let Ψ and Φ be a pair of quantum channels for which $\|(\Psi - \Phi)[|re^{i\phi}\rangle\langle re^{i\phi}|_{\text{coh}}]\| \leq \epsilon(\epsilon_0, r^2)$ for all r and for some concave (in r^2) function ϵ . Let ρ be any input state with average photon number \bar{n} . Then, for any $\kappa > 1$ and positive integer M ,*

$$\|(\Psi - \Phi)[\rho]\| \leq \left(1 - \frac{\bar{n}}{M}\right) \left(2(M+3)^M \kappa^{M-1} \epsilon\left(\epsilon_0, \frac{1}{\kappa}\right) + 4\sqrt{\frac{2\bar{n}}{\kappa M}}\right) + \frac{2\bar{n}}{M}. \quad (1)$$

This theorem has two free parameters, which must be tuned to attain the tightest bound. In particular, if we have $\epsilon(\epsilon_0, \tau) = \epsilon_0$ for $\tau < 1$ (i.e., τ is the energy of the coherent states we used to learn the channel in the first place), we could choose $\tau = \frac{1}{\kappa}$, so that the worst case scaling is approximately

$$\|(\Psi - \Phi)[\rho]\| \leq \mathcal{O}[e^{M \log(\frac{M}{\tau})} \tau \epsilon_0] + \mathcal{O}[\tau^{\frac{1}{2}} \bar{n}^{\frac{1}{2}} M^{-\frac{1}{2}}] + \mathcal{O}[\bar{n} M^{-1}]. \quad (2)$$

As ϵ_0 approaches 0, we can send $M \rightarrow \infty$ so that Eq. (1) approaches 0 too. If we also fix $M \sim \bar{n}$, we see that the error scales at most poly-exponentially in the input energy ($\sim \mathcal{O}[e^{\bar{n} \log(\bar{n})} \epsilon_0]$), so that a linear increase in the allowed \bar{n} (for fixed error) can be achieved with an exponential decrease in ϵ_0 .

In the specific case of a classical (but not necessarily coherent state) input, we get the corollary (proven in Appendix D):

Corollary 3.1 *Let ρ_{class} be a classical input state with average photon number \bar{n} . Then,*

$$\|(\Psi - \Phi)[\rho_{\text{class}}]\| \leq \epsilon(\epsilon_0, \bar{n}). \quad (3)$$

In the more general, but still not universal, case in which the input state has a finite negativity, \mathcal{N} , and a known P-representation, $P(re^{i\phi})$, we define the quantities:

$$\mu_P = 1 + 2\mathcal{N} = \iint |P(re^{i\phi})| r d\phi dr, \quad \nu_P = \iint |P(re^{i\phi})| r^3 d\phi dr, \quad \bar{n}_{\pm} = \frac{\iint P_{\pm}(re^{i\phi}) r^3 d\phi dr}{\iint P_{\pm}(re^{i\phi}) r d\phi dr}, \quad (4)$$

where P_{\pm} means we integrate over the positive/negative domain of P . Then, we have the corollary

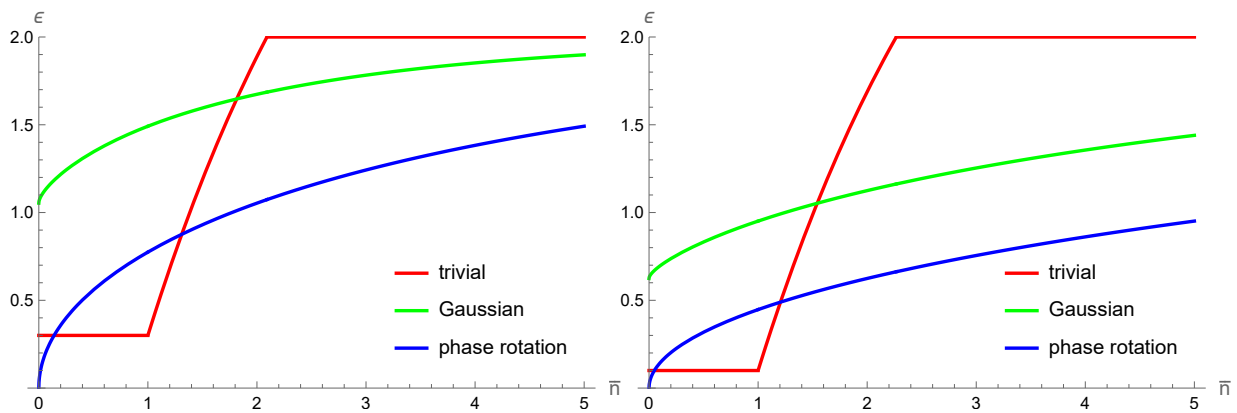


FIG. 2: Trace norm bounds as a function of the energy of the input coherent state using a variety of techniques. The red lines show the trivial, piecewise step function bound, the green lines show the bound for any pair of Gaussian channels, and the blue lines show the bound when both channels are phase rotations. In the plot on the left, we set $\epsilon_0 = 0.3$, whilst on the plot on the right, we set $\epsilon_0 = 0.1$. In both cases, $\tau^2 = 1$.

Corollary 3.2 *Let ρ_P be an input state with P -representation $P(re^{i\phi})$ and finite negativity \mathcal{N} . Then,*

$$\|(\Psi - \Phi)[\rho_P]\| \leq (1 + \mathcal{N})\epsilon(\epsilon_0, \bar{n}_+) + \mathcal{N}\epsilon(\epsilon_0, \bar{n}_-) \leq \mu_P \epsilon\left(\epsilon_0, \frac{\nu_P}{\mu_P}\right). \quad (5)$$

III. OUT-OF-DISTRIBUTION GENERALISATION FOR COHERENT STATES

Suppose two channels, Ψ and Φ , output similar output states for input coherent states in a given region. This similarity is quantified by $\|(\Psi - \Phi)[re^{i\phi}\langle re^{i\phi} |_{\text{coh}}]\| \leq \epsilon_0$ for $re^{i\phi}$ lying in some closed subset. We want to generalise this bound to every complex value of $re^{i\phi}$. For simplicity (and physical relevance), we assume the subset of coherent states over which we know Ψ and Φ are similar is a circle centred on the origin, so that the radius of the subset corresponds to the maximum average energy of the coherent states lying in it. Hence, our starting point is $\|(\Psi - \Phi)[re^{i\phi}\langle re^{i\phi} |_{\text{coh}}]\| \leq \epsilon_0$ for $r^2 \leq \tau^2$, and our goal is to find $\epsilon(\epsilon_0, r^2)$ such that $\|(\Psi - \Phi)[re^{i\phi}\langle re^{i\phi} |_{\text{coh}}]\| \leq \epsilon(\epsilon_0, r^2)$ for all r (with the inequality as tight as possible).

It is not necessarily the case that the channel outputs grow further apart as r increases. For instance, if Ψ and Φ are both replacement channels (i.e., channels that ignore the input and prepare some fixed output), the output distance will be constant for any input. The channel outputs could even converge for large r . However, in either of these scenarios, out-of-distribution generalisation is trivial, as we can simply define $\epsilon(\epsilon_0, r^2) = \epsilon_0$. We therefore focus on scenarios in which we expect $\epsilon(\epsilon_0, r^2)$ to grow with r . For instance, if Ψ and Φ are lossy channels, a small difference in the loss parameters will still result in similar outputs for low energy inputs, but the difference will grow with the energy of the inputs.

Trivially, we could choose the step function, $\epsilon_{\text{step}}(\epsilon_0, r^2)$, defined by

$$\epsilon_{\text{step}}(\epsilon_0, r^2) = \begin{cases} \epsilon_0 & r \leq \tau \\ 2 & r > \tau \end{cases}, \quad (6)$$

however this clearly gives us no out-of-distribution information. A slightly better choice would be to interpolate between the two regions, using the information processing inequality, which tells us that changing the input state by a distance of δ cannot increase the output distance by more than 2δ . Nonetheless, this improved form still lacks an important property: it is trivial for large r , even when $\epsilon_0 \rightarrow 0$. Hence, even if we gain perfect information about the subset of coherent states, the step function tells us nothing about large r . Theorem 1, which is a simple consequence of expressing the input state in a fixed basis (see Appendix B), tells us that at $\epsilon_0 = 0$, we should have $\epsilon(0, r^2) = 0$.

To be useful, the function $\epsilon(\epsilon_0, r^2)$ should be a decreasing function of ϵ_0 for every value of r^2 (i.e., we require that for any r and for $\epsilon'_0 < \epsilon_0$, $\epsilon(\epsilon'_0, r^2) \leq \epsilon(\epsilon_0, r^2)$). We also require it to approach 0 as ϵ_0 does so (i.e., for any r , $\epsilon(\epsilon_0, r^2) \rightarrow 0$ as $\epsilon_0 \rightarrow 0$). In theory, $\epsilon(\epsilon_0, r^2)$ could have an arbitrary dependence on r , since we only required it to be a decreasing function of ϵ_0 . However, given such a function with an arbitrary r -dependence, we can always construct $\epsilon'(\epsilon_0, r^2)$ as an upper concave hull of $\epsilon(\epsilon_0, r^2)$, i.e., a concave function (in terms of r^2) such that $\epsilon'(\epsilon_0, r^2) \geq \epsilon(\epsilon_0, r^2)$ for every value of r^2 . Thus, we will henceforth assume that our upper bound on the output trace norm for coherent states is an increasing and concave function of r^2 . Theorem 2 (proven in Appendix I using various concepts from later sections) tells us that it is always possible for us to find such a function.

If we know the classes of channel to which Ψ and Φ belong (for instance, if we know the general form of Ψ but are trying to learn specific channel parameters), we can find a function $\epsilon(\epsilon_0, r^2)$ by finding the worst case scenario set of errors in the parameters such that we still meet the constraint $\|(\Psi - \Phi)[|re^{i\phi}\rangle\langle re^{i\phi}|_{\text{coh}}]\| \leq \epsilon_0$ for $r^2 \leq \tau^2$. In Section VI, we demonstrate this for two example classes of channel.

In Fig. 2, we illustrate how we can construct various bounding functions based on the degree of knowledge we have about the channels. The trivial bound holds for every channel, but does not approach 0 for large \bar{n} , no matter how small we make ϵ_0 . If our target and learned channels are Gaussian, we can apply a tighter and always non-trivial bound (see Section VI A). If we know that we are looking for a phase rotation channel (i.e., the task is to learn the rotation parameter), we have a tighter bound still. Note that the non-trivial bounds are looser than the trivial bound in some regions; this is a consequence of the way they have been constructed. In particular, for phase rotation channels this is due to the looseness of the Fuchs-van de Graaf inequalities. Comparing the plots for $\epsilon_0 = 0.3$ and $\epsilon_0 = 0.1$, we see that improving the in-distribution error can greatly improve the out-of-distribution error. Whilst Fig. 2 refers to a specific scenario in which the channel we want to learn is a phase rotation, Theorem 2 tells us that a non-trivial bounding function always exists for small enough ϵ_0 .

IV. OUT-OF-DISTRIBUTION GENERALISATION FOR GENERAL STATES

Now assume we have a concave function $\epsilon(\epsilon_0, r^2)$ that bounds the distance between two channel outputs for any coherent state input. Our goal is to extend the bound to a general state input. Any state ρ can be represented as

$$\rho = \int P(\alpha)|\alpha\rangle\langle\alpha|_{\text{coh}}d^2\alpha = \int_0^\infty \int_0^{2\pi} P(re^{i\phi})|re^{i\phi}\rangle\langle re^{i\phi}|_{\text{coh}}rd\phi dr, \quad (7)$$

where we use $d^2\alpha$ to emphasise that this is a double integration over both the real and the imaginary component of α . The P-representation takes both positive and negative values, and is only positive-semidefinite for classical states.

We begin by considering a classical state with average photon number \bar{n} . That is, we have a state of the form in Eq. (7), but where the P-representation, $P_{\text{class}}(re^{i\phi})$, is constrained to be positive and to obey $\int_0^\infty r^2 \int_0^{2\pi} P_{\text{class}}(re^{i\phi})rd\phi dr \leq \bar{n}$. In Appendix D, we apply the convexity of the trace norm, the concavity of $\epsilon(\epsilon_0, r^2)$ (it is worth noting that concavity in r^2 is a looser condition than concavity in r), and Jensen's inequality to get the upper bound from Corollary 3.1:

$$\|(\Psi - \Phi)[\rho_{\text{class}}]\| \leq \epsilon(\epsilon_0, \bar{n}).$$

A. States with finite negativity

Now consider the more general case, in which the P-representation can take negative values. We can no longer immediately apply the convexity of the output trace norm. However, we can split ρ into two contributions:

$$\rho = \rho_+ - \rho_-, \quad \rho_+ = \int_{P(\alpha)>0} P(\alpha)|\alpha\rangle\langle\alpha|_{\text{coh}}d^2\alpha, \quad \rho_- = \int_{P(\alpha)<0} -P(\alpha)|\alpha\rangle\langle\alpha|_{\text{coh}}d^2\alpha, \quad (8)$$

where ρ_+ and ρ_- are given by integrating over the positive and negative domains, respectively, of the P-representation. They represent sub or super-normalised classical states. Defining $\mathcal{N} = \text{Tr}[\rho_-]$ (the negativity), we define

$$\sigma_+ = \frac{1}{1+\mathcal{N}}\rho_+, \quad \sigma_- = \frac{1}{\mathcal{N}}\rho_-. \quad (9)$$

Except for in the case of infinite negativity, these are now valid, classical quantum states, as they are normalised and have a positive overlap with every coherent state. From the linearity of quantum channels and using the triangle inequality, we write

$$\|(\Psi - \Phi)[\rho]\| = \|(1+\mathcal{N})(\Psi - \Phi)[\sigma_+] - \mathcal{N}(\Psi - \Phi)[\sigma_-]\| \leq (1+\mathcal{N})\|(\Psi - \Phi)[\sigma_+]\| + \mathcal{N}\|(\Psi - \Phi)[\sigma_-]\|. \quad (10)$$

We can then bound the trace norm of the outputs of the classical input states σ_+ and σ_- . Note that the average photon numbers of σ_\pm , \bar{n}_\pm , need not equal \bar{n} , the average photon number of ρ ; we only require $\bar{n} = (1+\mathcal{N})\bar{n}_+ - \mathcal{N}\bar{n}_-$. Applying Eq. (3),

$$\|(\Psi - \Phi)[\rho]\| \leq (1+\mathcal{N})\epsilon(\epsilon_0, \bar{n}_+) + \mathcal{N}\epsilon(\epsilon_0, \bar{n}_-). \quad (11)$$

Hence, from the P-representation of ρ , we can bound the distance of the learned channel output from the true channel output, using \mathcal{N} (which can be used as a measure of the non-classicality of the state [25]) and \bar{n}_\pm . Applying the concavity of function ϵ ,

$$\begin{aligned} (1+\mathcal{N})\epsilon(\epsilon_0, \bar{n}_+) + \mathcal{N}\epsilon(\epsilon_0, \bar{n}_-) &= (1+2\mathcal{N}) \left(\frac{1+\mathcal{N}}{1+2\mathcal{N}}\epsilon(\epsilon_0, \bar{n}_+) + \frac{\mathcal{N}}{1+2\mathcal{N}}\epsilon(\epsilon_0, \bar{n}_-) \right) \\ &\leq (1+2\mathcal{N})\epsilon \left(\epsilon_0, \frac{(1+\mathcal{N})\bar{n}_+ + \mathcal{N}\bar{n}_-}{1+2\mathcal{N}} \right) = \mu\epsilon \left(\epsilon_0, \frac{\nu}{\mu} \right), \end{aligned} \quad (12)$$

where we have defined the quantities $\mu = 1 + 2\mathcal{N}$ and $\nu = (1 + \mathcal{N})\bar{n}_+ + \mathcal{N}\bar{n}_-$. Eq. (11) provides a tighter bound, but Eq. (12) only requires knowledge of two quantities, rather than three, and will prove useful in the next subsection. Together, Eqs. (11) and (12) give Corollary 3.2.

B. States with infinite negativity

In general, \mathcal{N} can be infinite. Examples include Fock states and squeezed vacuum states. In this case, the bound in Eq. (11) becomes infinite, and hence trivial. The intuition we use to get around this is that every state with infinite negativity is δ -close to a state with finite (but potentially large) negativity. Suppose we have a state ρ with $\mathcal{N}(\rho) = \infty$. Then, for any small δ , we can find another state, σ , with finite negativity, such that $\|\rho - \sigma\| \leq \delta$. By the information processing inequality,

$$\|(\Psi - \Phi)[\rho]\| \leq \|(\Psi - \Phi)[\sigma]\| + 2\delta. \quad (13)$$

We can calculate $\|(\Psi - \Phi)[\sigma]\|$ using Eq. (12). As $\epsilon_0 \rightarrow 0$, $\|(\Psi - \Phi)[\sigma]\| \rightarrow 0$, but δ will remain fixed, so we will need to find another state with smaller δ but higher negativity.

Suppose we have a parametrised sequence of states $\{\sigma_s\}$, for $s \geq 0$, with distance δ_s from ρ and negativity \mathcal{N}_s , so that δ_s is an increasing function of s that starts at 0 for $s = 0$ and \mathcal{N}_s is a decreasing function of s that is finite for any $s \neq 0$. The average photon number for σ_s , \bar{n}_s , may differ from \bar{n} . Then we can decrease s as $\epsilon_0 \rightarrow 0$, so that we eventually converge to 0. For all s ,

$$\|(\Psi - \Phi)[\rho]\| \leq \mu_s \epsilon \left(\epsilon_0, \frac{\nu_s}{\mu_s} \right) + 2\delta_s. \quad (14)$$

The remaining task is therefore to find an appropriate sequence of states close to ρ . Taking the convolution of the P-representation of any state, $P(\alpha)[\rho]$, with $\frac{1}{s\pi} e^{-\frac{1}{s}|\alpha|^2}$ results in a new, valid state (for $s > 0$). In fact, if we set $s = \frac{1}{2}$ or $s = 1$, we get the W and Q-representations respectively of the original state. Since the Q-representation is always non-negative, this suggests the sequence of states with P-representations given by

$$P_s(\alpha)[\rho] = \rho_s = \frac{1}{s\pi} e^{-\frac{1}{s}|\alpha|^2} \star P(\alpha)[\rho] \quad (15)$$

could be useful for our purposes. For convenience, we define \mathcal{C}_s as the channel enacted by this convolution (this is equivalent to a Gaussian additive noise channel). In Appendix H, we show that, for this sequence, δ_s is upper bounded by

$$\delta_s \leq 2\sqrt{s(1 + 2\bar{n})}. \quad (16)$$

We know that, e.g., for the Fock states, any non-zero value of s has a finite negativity. However, this is not true in general: for squeezed vacuums, the negativity remains infinite up to some (squeezing dependent) threshold value, at which point it becomes 0. This threshold value is the non-classical depth for a squeezed vacuum state.

To make our sequence of states universal, we can therefore combine an energy truncation with convolution with channel \mathcal{C}_s . That is, we define $\sigma_{s,M} = \mathcal{C}_s(\rho^{(M)})$, with P-representation $P_{s,M}$, where $\rho^{(M)}$ is the truncation of ρ to an M -dimensional qudit state (i.e., applying a hard energy cutoff of $M - 1$ photons). We are free to choose any relationship between parameters s and M (so as to combine them into a single parameter) as long as $s \rightarrow 0$ when $M \rightarrow \infty$ (some later bounds will take $s \sim M^{-1}$).

Some care is required in defining the energy truncation: the truncation can be regarded as a channel that leaves an M -dimensional Hilbert space unchanged, but we have different options for how we treat the (higher energy) rest of the Hilbert space. For instance, we could map the rest of the Hilbert space to the vacuum state or we could map it to an erasure state, orthogonal to all number states. Whilst the first option is likely to give a slightly tighter bound, the erasure state option simplifies the calculations. Let η_M be the probability that a photon counting measurement on ρ gives a result of $M - 1$ or less. $\eta_M \rightarrow 1$ as $M \rightarrow \infty$ and it is bounded by $\eta_M \geq 1 - \frac{\bar{n}}{M}$. If we have a number state representation of ρ , we can also calculate η_M exactly as

$$\eta_M = \text{Tr}[\rho^{(M)}] = \sum_{m=0}^{M-1} \langle m|\rho|m\rangle. \quad (17)$$

Finally, we can write

$$\|(\Psi - \Phi)[\rho]\| \leq \eta_M \left(\mu_{s,M} \epsilon \left(\epsilon_0, \frac{\nu_{s,M}}{\mu_{s,M}} \right) + 2\delta_s \right) + 2(1 - \eta_M), \quad (18)$$

where we upper bound the error by assuming the channels are completely distinguishable on the erasure state (and so have an output trace norm of 2). In Appendices E and F, we show that the term $\mu_{s,M}\epsilon\left(\epsilon_0, \frac{\nu_{s,M}}{\mu_{s,M}}\right)$ can be upper bounded as

$$\mu_{s,M}\epsilon\left(\epsilon_0, \frac{\nu_{s,M}}{\mu_{s,M}}\right) \leq \mu_{s,M}^{(\text{UB})}\epsilon\left(\frac{s(1-s)(M+1)}{1-2s}\right), \quad (19)$$

where $\mu_{s,M}^{(\text{UB})}$ has an analytical expression, based on the number state decomposition of ρ , given in Eqs. (F15) and (F16). Crucially, Eq. (19) means that, for an appropriate scaling of s with M ($s \lesssim M^{-1}$), we can fix the argument of ϵ to a constant, eliminating our dependence on the specific form of function ϵ entirely. For a state ρ with known number state representation,

$$\|(\Psi - \Phi)[\rho]\| \leq \eta_M \left(\mu_{s,M}^{(\text{UB})}\epsilon\left(\epsilon_0, \frac{s(1-s)(M+1)}{1-2s}\right) + 4\sqrt{s(1+2\bar{n})} \right) + 2(1 - \eta_M). \quad (20)$$

On the other hand, if we have less information about the state (i.e., we only know the average energy and nothing about the form of the state), we can write a looser but even more general bound. In Appendix G, we show that for any $\kappa > 1$, we can write

$$\|(\Psi - \Phi)[\rho]\| \leq \left(1 - \frac{\bar{n}}{M}\right) \left(2(M+3)^M \kappa^{M-1} \epsilon\left(\epsilon_0, \frac{1}{\kappa}\right) + 4\sqrt{\frac{2\bar{n}}{\kappa M}} \right) + \frac{2\bar{n}}{M},$$

per Theorem 3. As previously shown (in Eq. 2), we can use a particular choice of κ to find the worst case scaling of the error.

Whilst this bound may be extremely loose (and exponential in M , so that even a fairly low M results in an error bound much larger than ϵ_0), it shows that out-of-distribution generalisation is always possible, for any input state, and with almost no prior knowledge about the input state (except for \bar{n}).

V. QUANTUM PROCESS TOMOGRAPHY, METROLOGY, AND MACHINE LEARNING INTERPRETATIONS OF CHANNEL LEARNING AND COMPARISON WITH EXISTING WORKS

The language and framing of our theorems is more typical of a ‘‘learning’’ framework than of metrology or process tomography, however this same problem is an important task in all three fields. Our results have general applicability, and so we set out here the connections between the various frameworks. However, this is not intended to be an exhaustive review of quantum machine learning, CV channel tomography, or quantum metrology.

First, let us describe the task of finding a bound of the form $\|(\Psi - \Phi)[|re^{i\phi}\rangle\langle re^{i\phi}|_{\text{coh}}]\| \leq \epsilon_0$ from a learning perspective. Φ could take the form of a physical device or process that we can choose optimal parameters for, but it could also simply represent our state of knowledge about the target. E.g., it could be a quantum process matrix or an equation, stored on a classical computer, that we can use to calculate the output state for a given input. The goal is to learn such a channel using a finite number, N , of sample states of the form $\Psi[|re^{i\phi}\rangle\langle re^{i\phi}|_{\text{coh}}]$ (where $r \leq \tau$). A learning algorithm might need multiple samples for each value of $re^{i\phi}$ as well as channel outputs for many different values of $re^{i\phi}$. On a quantum device, an algorithm of this type could work by using samples of both $\Psi[|re^{i\phi}\rangle\langle re^{i\phi}|_{\text{coh}}]$ and $\Phi[|re^{i\phi}\rangle\langle re^{i\phi}|_{\text{coh}}]$ (at the same points) to assess and bound $\|(\Psi - \Phi)[|re^{i\phi}\rangle\langle re^{i\phi}|_{\text{coh}}]\|$, over the region $r \leq \tau$, for a particular Φ and then evolve Φ to a new channel Φ' with a smaller output distance (using further samples from the target channel at each update step). This would be a form of quantum machine learning. If, instead, we only have a classical computer, we might perform tomography on all of our samples of $\Psi[|re^{i\phi}\rangle\langle re^{i\phi}|_{\text{coh}}]$ and then classically reconstruct Ψ by finding the learned channel, Φ , that best reproduces the measurement results amongst all channels in a certain class. These two scenarios are depicted in parts (a) and (b) of Fig. 1. In Appendix A, we take a brief look at the sample efficiency of possible measurements.

Working in the learning framework can provide us with useful tools for formulating guarantees on the output trace distance. If the ‘‘cost function’’ that we minimise is the maximum value of the output distance, evaluated over the training region, then we are immediately working in the formalism of our theorems. If the inputs are sampled randomly from the training region, we can apply in-distribution generalisation techniques [26–29] to bound (with high probability) the difference between the observed and true cost functions. Alternatively, we could choose the sampled inputs according to some fixed scheme that guarantees nowhere in the training region is far from a sampled point; bounds over the region would then follow from the data processing inequality.

In the language of quantum process tomography, characterising a quantum process involves learning the quantum process matrix that relates the elements of the input density matrix to the elements of the output density matrix in some basis. However, for a completely arbitrary CV channel, this matrix has infinite elements. A number of works have therefore developed the theory of coherent state quantum process tomography (csQPT) [4, 5, 30]. We will look in a little more detail at two foundational works.

The idea (as in this work) is to exploit the P-representation of Fock states in order to construct the process matrix. In Ref. [4], the process matrix is constructed by characterising the outputs for coherent state inputs ($\Psi[|\alpha\rangle\langle\alpha|_{\text{coh}}]$) and directly substituting them into the P-representations of the Fock state elements. The authors deal with the singularity of the P-representation by using

the Klauder approximation, which works similarly to the convolution with a Gaussian that we apply in Section IV B. Ref. [5] instead differentiates the Fock basis elements of $\Psi[|\alpha\rangle\langle\alpha|_{\text{coh}}]$ with regard to (the real and imaginary parts of) α . In both cases, a Fock basis truncation must be applied to the input state.

In both cases, the goal was to write the output of the channel as a function of its inputs. Here, instead, we assume we have such a function and want to rigorously bound its error. Indeed, the function could have been obtained by one of these methods. Hence, although a Fock decomposition of the input we want to know about may tighten our bounds, we do not need one in order to apply our theorems. Although the method in Section IV B also uses a Fock basis truncation, we also show how this truncation can be taken to infinity as our learning error, ϵ_0 , approaches 0.

Both papers do briefly mention errors, but only with regard to the additional errors introduced by their approximations/truncations. Hence, they ignore the fact that any measurements of the output states will themselves have non-zero errors; here we examine how our imperfect understanding of the channel even for the set of input states we do test propagates as we look at inputs outside of that set. In Ref. [4], interpolation is applied between the input states, to understand the behaviour for states that lie in-distribution but that were not previously sampled. Whilst this may be physically justified in many cases, a rigorous treatment of errors should bound the worst case scenario; our previous discussion of the learning framework gives examples of how this can be accomplished (in-distribution generalisation bounds or uniform sampling).

Another physically relevant framework is to see channel learning as a problem of parameter estimation. In many cases, the channel we want to learn about is not some completely arbitrary transformation. Rather, we may know it belongs to some parametrised class of channels and want to learn the (potentially many) parameters, which could represent some important information about a physical process. Examples could include the loss of a medium or the strength of some particular non-linear interaction. Quantum metrology then involves probing the channels in order to learn the parameter values. Errors in parameter estimation of $\mathcal{O}[N^{-\frac{1}{2}}]$ can be achieved using coherent states, and better error scalings are possible using clever strategies.

For the important class of Gaussian channels, protocols have been proposed that use csQPT to perform parameter estimation [31, 32]. One-mode Gaussian channels are fully characterised by a limited number of parameters and it is possible to learn all of them to within a small uncertainty.

The difficulty, from our perspective, is understanding how errors in the parameters translate to errors in output distance for arbitrary inputs. A small change in displacement is likely to have a drastically different effect on an arbitrary state than a similar magnitude change in a squeezing parameter. This is especially true if we consider non-Gaussian effects. Thus, a condition on the variance of whichever parameter we want to learn (often the goal in parameter estimation) does not automatically translate to a useful bound on the output distance of our target and learned channels. In Section VI, we illustrate via examples how knowledge about the output distance can be converted to bounds on the parameter difference and used to construct $\epsilon(\epsilon_0, r^2)$. This works both ways: for many channel classes, we may be able to convert a bound on the difference in parameters to the coherent state output distance and then apply our bounds for general states. This is the case regardless of how we estimated the parameters (i.e., even if we learned them using a different limited set of inputs to the low energy coherent states, such as a small number of non-coherent Gaussian probes [33, 34]), so our results are not limited to a specific model of quantum metrology.

We can connect parameter estimation to the idea of quantum machine learning. If we have an optical circuit that we want to imitate our target channel as closely as possible, we would do this by tuning the parameters of our circuit so that the outputs are as close to the target outputs as possible. We can view this as estimating the optimal parameters.

The precise form of the bound for low energy coherent state inputs that we use as our basic ingredient may not be the format in which the error of a sensing protocol is presented elsewhere. However, we chose this form for its generality, as any similar bound on the output distance can be rewritten in this way.

Finally, we note that our results are also of interest from a purely channel discrimination perspective (i.e., separately from both learning and quantum metrology).

VI. EXAMPLES: OUT-OF-DISTRIBUTION GENERALISATION FOR COHERENT STATES

We want to give analytical expressions for the function $\epsilon(\epsilon_0, r^2)$ for the case in which we have some prior knowledge about the target channel. The expressions necessarily depend on the specific forms of the target and learned channels, so to give more concrete statements, we focus on cases in which both belong to a certain parametrised class of channels. We therefore have target parameters and learned parameters, and the closer the two sets of parameters are, the closer the channels (and hence the channel outputs) will be. As specific examples, we will consider Gaussian channels and the cubic phase unitary.

A. Gaussian channels

A Gaussian channel transforms a Gaussian input with first moment vector q and covariance matrix V according to [3, 24]

$$q \rightarrow Mq + d, \quad V \rightarrow MVM^T + N, \quad (21)$$

where d is a 2-element real vector, M and N are 2 by 2 real matrices, $N = N^T \geq 0$, and $\det[N] \geq (\det[M] - 1)^2$ (we have adopted the convention that $\hbar = 2$). For the coherent state $|re^{i\phi}\rangle$, q has elements $2\text{Re}[re^{i\phi}] = 2r \cos(\phi)$ and $2\text{Im}[\alpha] = 2r \sin(\phi)$ and V is the identity matrix. For Gaussian channels \mathcal{G}_1 and \mathcal{G}_2 , characterised by d_i , M_i , and N_i , the output fidelity is [35]

$$F^2 = \frac{2 \exp[-\frac{1}{2}\mu^T(V_1 + V_2)^{-1}\mu]}{\sqrt{\Delta + \delta} - \sqrt{\delta}}, \quad \mu = (M_2 - M_1)q + (d_2 - d_1), \quad V_i = M_i M_i^T + N_i, \quad (22)$$

where $\delta = (\det[V_1] - 1)(\det[V_2] - 1)$ and $\Delta = \det[V_1 + V_2]$. Examining the r -dependence, we can see F^2 is the exponential of a quadratic in r . Letting x , y , and z be some unknown functions of d_i , M_i , N_i , and ϕ , the output fidelity can be expressed as

$$F^2 = x e^{-(yr^2 + zr)} \leq x e^{-yr^2 + |z|r}, \quad (23)$$

where we have folded the angular dependence of the outputs into the definitions of parameters x , y , and z . This form holds for every pair of Gaussian channels, so our goal is simply to bound x , y , and z .

If we know $\|(\mathcal{G}_1 - \mathcal{G}_2)[|re^{i\phi}\rangle\langle re^{i\phi}|_{\text{coh}}]\| \leq \epsilon_0$ for all ϕ and for $r \leq \tau$, we can lower bound x and upper bound y and $|z|$. Hence, we can lower bound F^2 and so, via the Fuchs-van de Graaf inequality [36], upper bound the output distance. Specifically,

$$x \geq \left(\frac{2 - \epsilon_0}{2}\right)^2, \quad y \leq \frac{2}{\tau^2} \log \left[\frac{2}{2 - \epsilon_0}\right], \quad |z| \leq \frac{1}{\tau} \log \left[\frac{2}{2 - \epsilon_0}\right], \quad (24)$$

where we obtain the bounds by assessing Eq. (23) at $r = 0$ and $r = \pm\tau$ (strictly, $r \geq 0$ but for simplicity we treat $\phi \rightarrow \phi + \pi$ as $r \rightarrow -r$) and comparing the resulting expressions to our condition. Note that the three expressions in Eq. (24) cannot all be saturated simultaneously for our condition to hold, but they allow us to lower bound Eq. (23) for every value of r . We get

$$F^2 \leq \left(\frac{2 - \epsilon_0}{2}\right)^{2\frac{r^2}{\tau^2} + \frac{r}{\tau} + 2}, \quad \|(\mathcal{G}_1 - \mathcal{G}_2)[|re^{i\phi}\rangle\langle re^{i\phi}|_{\text{coh}}]\| \leq \epsilon_{\text{Gaussian}}(\epsilon_0, r^2) = 2\sqrt{1 - \left(\frac{2 - \epsilon_0}{2}\right)^{2\frac{r^2}{\tau^2} + \frac{r}{\tau} + 2}}, \quad (25)$$

which we immediately see obeys the property of convergence to 0 as $\epsilon_0 \rightarrow 0$. Notably, it is never trivial (greater than 2) for large r and is concave in r^2 (though not in r). However, it can be significantly higher than ϵ_0 even in the $r < \tau$ region (so is trivial in this region). This is the price we pay for bounding x , y , and z individually; we could potentially get a tighter bound by working directly with Eq. (23) to construct a (possibly piecewise) bound. Further calculation details are given in Appendix C.

If we specify more details about the forms of the Gaussian channels under consideration, we may be able to do better. As an example, we consider some single-parameter Gaussian unitaries. For an unknown displacement, the output fidelity is independent of the input coherent state, so $\epsilon_{\text{dis}}(\epsilon_0, r^2) = \epsilon_0$. For learning an unknown phase rotation,

$$\epsilon_{\text{PR}}(\epsilon_0, r^2) = 2\sqrt{1 - \left(\frac{2 - \epsilon_0}{2}\right)^{\frac{r^2}{\tau^2}}}. \quad (26)$$

For single-mode squeezing,

$$\epsilon_{\text{sq}}(\epsilon_0, r^2) = 2\sqrt{1 - \frac{1}{2\tau^2} W_0[e^{2\tau^2} \tau^2 (2 - \epsilon_0)] \exp\left[r^2 \left(\frac{1}{\tau^2} W_0[e^{2\tau^2} \tau^2 (2 - \epsilon_0)] - 2\right)\right]}, \quad (27)$$

where W_0 is the Lambert W function. As another example, suppose the channels are rotationally symmetric (no angular dependence), as is the case for a range of channel classes, including lossy channels and quantum-limited amplifiers. Then we have $z = 0$, so we get the tighter bound

$$\epsilon_{\text{sym}}(\epsilon_0, r^2) = 2\sqrt{1 - \left(\frac{2 - \epsilon_0}{2}\right)^{2\left(\frac{r^2}{\tau^2} + 1\right)}}. \quad (28)$$

Note that all four expressions are concave in r^2 and that they tend to 0 as $\epsilon_0 \rightarrow 0$.

B. Cubic phase unitary

The cubic phase gate is an important gate in CV quantum computing, because it is one option for the non-Gaussian operation required to make CV quantum computing universal [3]. It applies the unitary $V_\gamma = e^{i\gamma\hat{q}^3}$, where q is one of the quadratures of a CV mode. To understand how it transforms a coherent state, it is easiest to work in the \hat{q} basis. Specifically, we write

$$|\alpha\rangle = \frac{1}{\sqrt{2\pi}} \int_{-\infty}^{\infty} \exp\left[-\frac{(q - 2\text{Re}[\alpha])^2}{4} + i(q - 2\text{Re}[\alpha])\text{Im}[\alpha]\right] |q\rangle dq, \quad (29)$$

where $\{|q\rangle\}$ are the (unnormalisable) eigenstates of the \hat{q} operator. The output fidelity between operations V_β and V_γ is then

$$|\langle\alpha|V_\beta^\dagger V_\gamma|\alpha\rangle| = \frac{1}{\sqrt{2\pi}} \left| \int_{-\infty}^{\infty} e^{i(\gamma-\beta)q^3 - \frac{1}{2}(q-2\text{Re}[\alpha])^2} dq \right|. \quad (30)$$

This integral is difficult to evaluate analytically, but numerically we find that it is a decreasing function of $\Delta_\gamma = |\gamma - \beta|$ and of (the real part of) α . To understand why, consider that Eq. (30) is the convolution of the Gaussian function $(2\pi)^{-\frac{1}{2}} e^{-\frac{1}{2}q^2}$ (which integrates to 1) and the oscillatory function $e^{i\Delta_\gamma q^3}$ at the point $2\text{Re}[\alpha]$. As q (or Δ_γ) gets larger, the oscillations become more frequent, so the integral over a small locality becomes approximately zero (the positive and negative contributions cancel out). If the Gaussian function is centred in the slowly oscillating region (i.e., if $\text{Re}[\alpha]$ is small), then the contributions will not cancel out much and the magnitude of the integral will be close to 1. For large $\text{Re}[\alpha]$, the integral will be closer to 0. As we may expect, the output fidelity is independent of $\text{Im}[\alpha]$, but since we want to bound the output distance over all coherent states in the region, we must choose $\alpha = \text{Re}[\alpha]$. If we are guaranteed that, for some τ , $\|(\Psi - \Phi)[|\tau e^{i\phi}\rangle\langle\tau e^{i\phi}|_{\text{coh}}]\| \leq \epsilon_0$, we can numerically upper bound Δ_γ , and so can construct a function $\epsilon(\epsilon_0, r^2)$ such that $\|(\Psi - \Phi)[|r e^{i\phi}\rangle\langle r e^{i\phi}|_{\text{coh}}]\| \leq \epsilon(\epsilon_0, r^2)$ for all r .

VII. EXAMPLES: OUT-OF-DISTRIBUTION GENERALISATION FOR GENERAL STATES

We will consider three different types of non-classical input state, to demonstrate how the various bounds can be applied: single-photon-added thermal states (SPATs), Fock states, and one-mode squeezed vacuums. SPATs have a finite negativity. Fock states have infinite negativity for any non-zero energy, but this negativity becomes finite with convolution alone (without the need for an energy truncation). Squeezed vacuums require both truncation and convolution to reach finite negativity.

A. Single-photon-added thermal states

SPATs have the P-representation [37]

$$P_{\text{SPAT}}(r e^{i\phi}) = \frac{1+q}{\pi q^3} \left(r^2 - \frac{q}{1+q} \right) e^{-\frac{r^2}{q}}, \quad (31)$$

where $q > 0$ is the average photon number of the thermal state before the photon addition (a conditional process, involving post-selection). q is connected to the average photon number of the SPAT by $\bar{n} = 1 + 2q$. From Eq. (31), we can see that the P-representation has no angular dependence and starts negative for small r before becoming positive for $r^2 > \frac{q}{1+q} = \frac{\bar{n}-1}{\bar{n}+1}$. We can explicitly calculate \mathcal{N} and \bar{n}_\pm :

$$\mathcal{N} = e^{-\frac{1}{1+q}} \left(1 + \frac{1}{q} \right) - 1, \quad \bar{n}_- = 1 + 2q - \frac{1}{1 + \left(1 - e^{-\frac{1}{1+q}} \right) q}, \quad \bar{n}_+ = 1 + 2q - \frac{1}{1+q}. \quad (32)$$

We could then use the bound in Eq. (11). We can also simplify our calculations by instead using the bound in Eq. (12), with

$$\mu = 2e^{-\frac{1}{1+q}} \frac{1+q}{q} - 1, \quad \frac{\nu}{\mu} = 1 + 2q - \frac{2}{2 + 2q - e^{-\frac{1}{1+q}} q} < 1 + 2q. \quad (33)$$

The bound becomes

$$\|(\Psi - \Phi)[\rho_{\text{SPAT}}]\| \leq \left(2e^{-\frac{1}{1+q}} \frac{1+q}{q} - 1 \right) \epsilon \left(\epsilon_0, 1 + 2q - \frac{2}{2 + 2q - e^{-\frac{1}{1+q}} q} \right). \quad (34)$$

Since $\bar{n}_- < \frac{\nu}{\mu} < \bar{n}_+$, Eq. (34) is no more than a factor of $\frac{\mu}{\mu-1} = 2 - e^{-\frac{1}{1+q}} \frac{q}{1+q}$ looser than the bound from Eq. (11).

The quantity $\frac{\nu}{\mu}$ increases approximately linearly with \bar{n} (or k). Since the function ϵ is concave, $\epsilon(\epsilon_0, \frac{\nu}{\mu})$ increases sublinearly with the energy of the SPAT. On the other hand, the negativity diverges for small \bar{n} ; this is to be expected as the limiting case of $\bar{n} \rightarrow 1$ ($k \rightarrow 0$) is the Fock state $|1\rangle\langle 1|$. The overall bound on the closeness of the two channel outputs for an input SPAT is therefore larger for lower energies (but higher non-classicalities). It should be noted that the bound being larger does not necessarily imply the channel outputs are further away; the bound may simply be looser for such inputs. As briefly discussed in Appendix J, it may be possible to apply the technique from Section IV B of using a sequence of states with lower negativities in order to tighten the bounds somewhat.

B. Fock states

The Fock state $|m\rangle\langle m|$ has the P-representation

$$P_{s,\text{Fock}}(r e^{i\phi}) = \frac{(-1)^m (1-s)^m}{\pi s^{m+1}} e^{-\frac{1}{s}r^2} L_m \left[\frac{r^2}{s(1-s)} \right]. \quad (35)$$

In Appendix F, we show that the values of the relevant quantities are

$$\mu_s^{(\text{UB})} = 2 \frac{(1-s)^{m+1}}{s^m(1-2s)}, \quad \nu_s^{(\text{UB})} = 4 \frac{(1-s)^{m+2}}{s^{m-1}(1-2s)^2}, \quad (36)$$

so that the bound in Eq. (14) becomes

$$\|(\Psi - \Phi)[|m\rangle\langle m|]\| \leq 2 \frac{(1-s)^{m+1}}{s^m(1-2s)} \epsilon \left(\epsilon_0, \frac{2s(1-s)}{1-2s} \right) + 4\sqrt{s(1+2m)}. \quad (37)$$

The first term is exponential in the energy of the Fock state, since it is proportional to $(\frac{1-s}{s})^m$, whilst the second term is sublinear in m . The s -dependence is less straightforward, and depends on the form of ϵ , but the multiplicative factor quickly becomes large for small s and $m > 0$.

C. One-mode squeezed vacuums

A one-mode squeezed vacuum with squeezing parameter $r = \text{arctanh}(\lambda)$ (and average photon number $\bar{n} = \sinh(r)^2 = \frac{\lambda^2}{1-\lambda^2}$) has density matrix [3]

$$\rho_{\text{sq}} = \sqrt{1-\lambda^2} \sum_{p,q=0}^{\infty} \frac{\lambda^{p+q} \sqrt{(2p)!(2q)!}}{2^{p+q} p! q!} |2p\rangle\langle 2q|. \quad (38)$$

If $s > \frac{\lambda}{1+\lambda}$, then $\mathcal{N} = 0$. Otherwise, in Appendix K, we show that μ is upper bounded by

$$\mu_{s,M}^{(\text{UB})} = \frac{2(1-s)\sqrt{1-\lambda^2}}{(1-2s)} \left(\frac{4(y_1^{\frac{M+1}{2}} - 1)}{\pi \sqrt{(1+x)}(y_1 - 1)} + \frac{y_2^{\frac{M+1}{2}} - 1}{y_2 - 1} \right), \quad (39)$$

$$y_1 = \frac{\lambda(1-s)(1+x)}{s(1-2s)}, \quad y_2 = \frac{\lambda(1-s)x}{s(1-2s)}, \quad x = \frac{(1-2s)(1-s)\lambda}{s}. \quad (40)$$

Note that the approximate scaling of the negativity with s , M , and λ (for $s \ll \frac{\lambda}{1+\lambda}$) is $\mathcal{O}[\lambda^{M-1} s^{1-M}]$. η_M evaluates to

$$\eta_M = \sqrt{1-\lambda^2} \sum_{p=0}^{\frac{M-1}{2}} \frac{\lambda^{2p} (2p)!}{4^p (p!)^2} = 1 - \frac{\beta[\lambda^2; \frac{M+1}{2}, \frac{1}{2}] \Gamma[\frac{M}{2} + 1]}{\sqrt{\pi} (\frac{M-1}{2})!} \leq 1 - \frac{\lambda^2}{M(1-\lambda^2)}, \quad (41)$$

where β is the incomplete beta function. The exact value is easy to calculate numerically for a specific value of M , whilst the bound can be used for a simpler analytic expression. We can then construct a piecewise bound, with

$$\|(\Psi - \Phi)[\rho_{\text{sq}}]\| \leq \epsilon \left(\epsilon_0, \frac{\lambda^2}{1-\lambda^2} + s \right) + 4\sqrt{s \frac{1+\lambda^2}{1-\lambda^2}} \quad \text{for } s > \frac{\lambda}{1+\lambda} \quad (42)$$

and Eq. (20) (substituting in Eqs. (39) and (41)) otherwise.

VIII. CONCLUSION

When learning the action of a quantum channel, it is often not possible to test every possible input state. Instead, we can aim to find a learned channel that reproduces the input-output relations for simple, low energy, classical probes. We want to be sure that this learned channel also reproduces the input-output relations for higher energy and non-classical inputs.

In this paper, we have shown that a bound on the distance of between the outputs of two channels for low energy coherent state inputs can always give rise to a bound on the output distance for higher energy coherent state inputs, as long as the initial bound is tight enough. Such a bound, in turn, gives rise to a bound on the output distance for all input states. This bound converges to 0 as the output distance for coherent state inputs converges to 0. This is a useful result – with implications for subjects such as quantum machine learning and quantum metrology, amongst others – as it shows that it is sufficient to probe a process with experimentally simple, classical probes. We have given general statements that hold for all classes of channel and for all input states, as well as looking at specific, useful examples of channel classes and types of input state.

One avenue for future research is to extend this result from one-mode channels to multi-mode channels and to formulate bounds that account for idler modes. Another option would be to look at other specific classes of channels or input states. Many of the existing bounds could also be tightened. Finally, it would be useful to bound the worst case scaling of the function ϵ with r^2 ; in this work we have only demonstrated that there exists an ϵ that approaches 0 as ϵ_0 approaches 0.

Acknowledgments

The authors acknowledge financial support from: CLUSTEC, which has received funding from the European Union’s Horizon Europe programme, under grant agreement No. 101080173 (J.L.P.); NGI Enrichers, which has received funding from the European Union’s Horizon Europe Research and Innovation Programme, under grant agreement 101070125 (J.L.P.); U.S. Department of Energy, Office of Science, National Quantum Information Science Research Centers, Superconducting Quantum Materials and Systems Center (SQMS), under the Contract No. DE-AC02-07CH11359 (J.L.P., Q.Z. and L.B.); PNRR Ministero Università e Ricerca Project No. PE0000023-NQSTI, funded by European Union-Next-Generation EU (L.B.); Prin 2022 - DD N. 104 del 2/2/2022, entitled “understanding the LEarning process of QUantum Neural networks (LeQun)”, proposal code 2022WHZ5XH, CUP B53D23009530006 (L.B.); the European Union’s Horizon Europe research and innovation program under EPIQUE Project GA No. 101135288 (L.B.). Q.Z. also acknowledges support from NSF (CCF-2240641, OMA-2326746, 2350153), ONR (N00014-23-1-2296), AFOSR MURI FA9550-24-1-0349 and DARPA (MeasQUIT HR0011-24-9-0362, HR00112490453, HR001123S0052). Part of the work was carried out during J.L.P.’s research visit to USC. J.L.P. also thanks Matteo Paris for helpful discussions.

-
- [1] V. Gebhart, R. Santagati, A. A. Gentile, E. M. Gauger, D. Craig, N. Ares, L. Banchi, F. Marquardt, L. Pezzè, and C. Bonato, *Nature Reviews Physics* **5**, 141 (2023).
 - [2] S. L. Braunstein and P. Van Loock, *Reviews of modern physics* **77**, 513 (2005).
 - [3] C. Weedbrook, S. Pirandola, R. García-Patrón, N. J. Cerf, T. C. Ralph, J. H. Shapiro, and S. Lloyd, *Reviews of Modern Physics* **84**, 621 (2012).
 - [4] M. Lobino, D. Korystov, C. Kupchak, E. Figueroa, B. C. Sanders, and A. I. Lvovsky, *Science* **322**, 563 (2008).
 - [5] S. Rahimi-Keshari, A. Scherer, A. Mann, A. T. Rezakhani, A. I. Lvovsky, and B. C. Sanders, *New J. Phys.* **13**, 013006 (2011), ISSN 1367-2630.
 - [6] M. Cooper, E. Slade, M. Karpiński, and B. J. Smith, *New J. Phys.* **17**, 033041 (2015), ISSN 1367-2630.
 - [7] M. Kervinen, S. Ahmed, M. Kudra, A. Eriksson, F. Quijandría, A. F. Kockum, P. Delsing, and S. Gasparinetti, *Phys. Rev. A* **110**, L020401 (2024).
 - [8] M. C. Caro, H.-Y. Huang, N. Ezzell, J. Gibbs, A. T. Sornborger, L. Cincio, P. J. Coles, and Z. Holmes, *Nat Commun* **14**, 3751 (2023), ISSN 2041-1723.
 - [9] Y. Zhang, R. Wiersema, J. Carrasquilla, L. Cincio, and Y. B. Kim, *Scalable quantum dynamics compilation via quantum machine learning* (2024), 2409.16346.
 - [10] B.-B. Li, L. Ou, Y. Lei, and Y.-C. Liu, *Nanophotonics* **10**, 2799 (2021).
 - [11] Y. Xia, A. R. Agrawal, C. M. Pluchar, A. J. Brady, Z. Liu, Q. Zhuang, D. J. Wilson, and Z. Zhang, *Nature Photonics* **17**, 470 (2023).
 - [12] A. J. Brady, X. Chen, Y. Xia, J. Manley, M. Dey Chowdhury, K. Xiao, Z. Liu, R. Harnik, D. J. Wilson, Z. Zhang, et al., *Communications Physics* **6**, 237 (2023).
 - [13] A. Eickbusch, V. Sivak, A. Z. Ding, S. S. Elder, S. R. Jha, J. Venkatraman, B. Royer, S. M. Girvin, R. J. Schoelkopf, and M. H. Devoret, *Nature Physics* **18**, 1464 (2022).
 - [14] Y. Xia, W. Li, W. Clark, D. Hart, Q. Zhuang, and Z. Zhang, *Physical Review Letters* **124**, 150502 (2020).
 - [15] Q. Zhuang and J. H. Shapiro, *Physical review letters* **128**, 010501 (2022).
 - [16] I. Coddington, N. Newbury, and W. Swann, *Optica* **3**, 414 (2016).
 - [17] H. Shi, Z. Chen, S. E. Fraser, M. Yu, Z. Zhang, and Q. Zhuang, *npj Quantum Information* **9**, 91 (2023).
 - [18] A. Hariri, S. Liu, H. Shi, Q. Zhuang, X. Fan, and Z. Zhang, arXiv:2412.19800 (2024).
 - [19] D. I. Herman, M. Walsh, M. K. Kreider, N. Lordi, E. J. Tsao, A. J. Lind, M. Heyrich, J. Combes, J. Genest, and S. A. Diddams, arXiv preprint arXiv:2408.16688 (2024).

- [20] W. Kozłowski and S. Wehner, in *Proceedings of the sixth annual ACM international conference on nanoscale computing and communication* (2019), pp. 1–7.
- [21] H. Shi, Z. Zhang, and Q. Zhuang, *Physical Review Applied* **13**, 034029 (2020).
- [22] Y. Shen, N. C. Harris, S. Skirlo, M. Prabhu, T. Baehr-Jones, M. Hochberg, X. Sun, S. Zhao, H. Larochelle, D. Englund, et al., *Nature photonics* **11**, 441 (2017).
- [23] P. Kok, W. J. Munro, K. Nemoto, T. C. Ralph, J. P. Dowling, and G. J. Milburn, *Reviews of modern physics* **79**, 135 (2007).
- [24] A. Serafini, *Quantum continuous variables: a primer of theoretical methods* (CRC press, 2023).
- [25] K. C. Tan, S. Choi, and H. Jeong, *Phys. Rev. Lett.* **124**, 110404 (2020).
- [26] S. Arunachalam and R. de Wolf, *A Survey of Quantum Learning Theory* (2017), 1701.06806.
- [27] H.-Y. Huang, M. Broughton, M. Mohseni, R. Babbush, S. Boixo, H. Neven, and J. R. McClean, *Nat Commun* **12**, 2631 (2021), ISSN 2041-1723.
- [28] L. Bianchi, J. Pereira, and S. Pirandola, *PRX Quantum* **2**, 040321 (2021).
- [29] M. C. Caro, H.-Y. Huang, M. Cerezo, K. Sharma, A. Sornborger, L. Cincio, and P. J. Coles, *Nat Commun* **13**, 4919 (2022), ISSN 2041-1723.
- [30] A. Anis and A. I. Lvovsky, *New J. Phys.* **14**, 105021 (2012), ISSN 1367-2630.
- [31] X.-B. Wang, Z.-W. Yu, J.-Z. Hu, A. Miranowicz, and F. Nori, *Phys. Rev. A* **88**, 022101 (2013).
- [32] Y. S. Teo, K. Park, S. Shin, H. Jeong, and P. Marek, *New J. Phys.* **23**, 063024 (2021), ISSN 1367-2630.
- [33] M. Bina, F. Grasselli, and M. G. A. Paris, *Phys. Rev. A* **97**, 012125 (2018).
- [34] A. Candeloro, S. Razavian, M. Piccolini, B. Teklu, S. Olivares, and M. G. A. Paris, *Entropy* **23**, 1353 (2021), ISSN 1099-4300.
- [35] L. Bianchi, S. L. Braunstein, and S. Pirandola, *Physical review letters* **115**, 260501 (2015).
- [36] M. A. Nielsen and I. L. Chuang, *Quantum Computation and Quantum Information: 10th Anniversary Edition* (Cambridge University Press, USA, 2010), 10th ed., ISBN 978-1-107-00217-3.
- [37] T. Kiesel, W. Vogel, V. Parigi, A. Zavatta, and M. Bellini, *Phys. Rev. A* **78**, 021804 (2008).
- [38] A. I. Lvovsky and M. G. Raymer, *Rev. Mod. Phys.* **81**, 299 (2009).
- [39] O. Landon-Cardinal, L. C. G. Góvia, and A. A. Clerk, *Phys. Rev. Lett.* **120**, 090501 (2018).
- [40] M. Kalash and M. V. Chekhova, *Optica, OPTICA* **10**, 1142 (2023), ISSN 2334-2536.
- [41] Y.-D. Wu, Y. Zhu, G. Chiribella, and N. Liu, *Phys. Rev. Res.* **6**, 033280 (2024).
- [42] F. A. Mele, A. A. Mele, L. Bittel, J. Eisert, V. Giovannetti, L. Lami, L. Leone, and S. F. E. Oliviero, *Learning quantum states of continuous variable systems* (2024), 2405.01431.
- [43] C.-H. Nguyen, K.-W. Tseng, G. Maslennikov, H. C. J. Gan, and D. Matsukevich, *Experimental SWAP test of infinite dimensional quantum states* (2021), 2103.10219.
- [44] I. Pietikäinen, O. Černotík, S. Puri, R. Filip, and S. M. Girvin, *Quantum Sci. Technol.* **7**, 035025 (2022), ISSN 2058-9565.
- [45] T. J. Volkoff and Y. Subaşı, *Quantum* **6**, 800 (2022).
- [46] S. Lloyd, M. Schuld, A. Ijaz, J. Izaac, and N. Killoran, *Quantum embeddings for machine learning* (2020), 2001.03622.
- [47] S. Lloyd, M. Mohseni, and P. Rebentrost, *Nature Phys* **10**, 631 (2014), ISSN 1745-2481.
- [48] L. Bianchi, J. L. Pereira, S. T. Jose, and O. Simeone, *Adv. Quantum Technol.* **n/a**, 2300311 (2024), ISSN 2511-9044.
- [49] A. Wuensche, *Acta Physica Slovaca* **48**, 385 (1998), ISSN 0323-0465.

Appendix A: Measurements of the outputs

Let us consider how we can assess $\|(\Psi - \Phi)[|re^{i\phi}\rangle\langle re^{i\phi}|_{\text{coh}}]\|$ for a particular value of $re^{i\phi}$. One option is to carry out tomography on our copies of $\Psi[|re^{i\phi}\rangle\langle re^{i\phi}|_{\text{coh}}]$ (up to some trace norm error η) and then assess the output distance classically. Another option, if we are carrying out the learning algorithm using a quantum device capable of producing copies of $\Phi[|re^{i\phi}\rangle\langle re^{i\phi}|_{\text{coh}}]$, is to directly measure $\|(\Psi - \Phi)[|re^{i\phi}\rangle\langle re^{i\phi}|_{\text{coh}}]\|$, without explicitly obtaining classical descriptions of the output states.

There exist a variety of methods for performing tomography on CV states, some of which are specific to certain types of state. Some more general methods involve the reconstruction of the Husimi Q-function or the Wigner function by applying homodyne, heterodyne, or other measurements, after displacing, squeezing, or otherwise operating on the state [38–40]. If we know the output states have a property called reflection symmetry, we can estimate their characteristic function at several points [41]. If we know the outputs are Gaussian states, we need only accurately learn their first and second moments in order to fully characterise them. In Ref. [42], it is shown that we need only learn these moments up to $\mathcal{O}[\eta^2]$, and explicit bounds on the trace distance between Gaussian states are given, based on the difference in first and second moments and the average energies of the states.

The downside of tomography based methods is that they can be extremely inefficient for CV states. Even for pure states, one requires $S = \mathcal{O}[E\eta^{-2}]$ copies for tomography of a non-Gaussian output, and at least $S = \mathcal{O}[E^2\eta^{-2}]$ copies (at most $S = \mathcal{O}[E^2\eta^{-3}]$ copies) are required for mixed states [42]. Here, E is the average energy of the output that we want to characterise. Crucially, this is not necessarily the same as r^2 , the energy of the input coherent state, and could, depending on the target channel, be much higher (and also may not be known a priori). Note that the error in estimation, η , must be added to the assessed value of $\|(\Psi - \Phi)[|re^{i\phi}\rangle\langle re^{i\phi}|_{\text{coh}}]\|$, when formulating the bound.

For pure output states, a direct assessment of the output distance can be accomplished using the SWAP test. The SWAP test is a two-outcome measurement on a pair of states, ψ_1 and ψ_2 , that outputs 0 with probability $\frac{1}{2} + \frac{1}{2}\text{Tr}[\psi_1\psi_2]$. If the outputs, $\Psi[|re^{i\phi}\rangle\langle re^{i\phi}|_{\text{coh}}]$ and $\Phi[|re^{i\phi}\rangle\langle re^{i\phi}|_{\text{coh}}]$, are pure, this immediately tells us their squared fidelity, up to an error of $\mathcal{O}[\sqrt{S^{-1}}]$.

Applying the Fuchs-van de Graaf relation, we get $S = \mathcal{O}[\eta^2]$. Though this error scaling may seem similar to the tomography expressions, a crucial difference is that it is entirely independent of the energy of the output state.

The SWAP test can be enacted using a controlled beamsplitter [43, 44]. However, this is a non-Gaussian component, and so may be difficult to implement. In Ref. [45], it is shown that the SWAP test can be implemented in the CV setting using only linear optics and photon counting. Thus, for unitary Ψ and Φ , we can assess the output distance using just a single beamsplitter and photon counters (although the finite threshold of any real photon counter will introduce errors).

For mixed state outputs, the SWAP test only lets us learn the overlap of $\Psi[|re^{i\phi}\rangle\langle re^{i\phi}|_{\text{coh}}]$ and $\Phi[|re^{i\phi}\rangle\langle re^{i\phi}|_{\text{coh}}]$. This would not give a bound on the output distance that converges to 0 when the target and learned channels coincide. One alternative is to use the implementation of the Helstrom measurement from Ref. [46]. This method is based on the state exponentiation algorithm [47] and phase estimation, and it uses copies of (unknown) states ψ_1 and ψ_2 to apply the optimal discriminator between ψ_1 and ψ_2 to an arbitrary state. In Ref. [48], it was shown that enacting the Helstrom measurement on a single state with a failure probability of ζ requires $S = \mathcal{O}[-\log(\zeta)\zeta^{-3}]$ copies of each state. Since the optimal measurement should correctly discriminate between the states with a probability linear in the trace distance (in fact, this is precisely its operational meaning), we could estimate the output distance by applying the Helstrom measurement to multiple copies of the output states and finding the error probability. To estimate it to error probability $\mathcal{O}[\zeta]$ (so that the two contributors to the error are equal), we would carry out the protocol $\sim \zeta^{-2}$ times, and so the total number of copies required is $S = \mathcal{O}[-\log(\zeta)\zeta^{-5}]$. At first glance, this is quite costly, but the complete lack of dependence on the output states themselves (including the lack of dependence on E) could make this algorithm more efficient than tomography, in some circumstances. In terms of implementation, however, this would require many uses of a controlled beamsplitter, and so would not be practical for near-term applications.

Appendix B: Out-of-distribution generalisation for coherent states when $\epsilon_0 = 0$

We want to show that if two channels (i.e., the target channel and the learned channel) have exactly the same output for low energy coherent state inputs, then they must also have the same output for any coherent state input. More precisely, suppose $\|(\Psi - \Phi)[|re^{i\phi}\rangle\langle re^{i\phi}|_{\text{coh}}]\| = 0$ for $r \leq \tau$. Then, this holds for $r > \tau$ too. Whilst intuitive, this is worth proving, since it guarantees that if we learn a channel exactly over a small area of the phase space, we have also learned it over all of phase space.

If $\|(\Psi - \Phi)[|re^{i\phi}\rangle\langle re^{i\phi}|_{\text{coh}}]\| = 0$ for $r \leq \tau$, then

$$e^{-r^2} \left\| \sum_{m,n=0}^{\infty} \frac{r^{m+n} e^{i(m-n)\phi}}{\sqrt{m!n!}} (\Psi - \Phi)[|m\rangle\langle n|] \right\| = 0 \quad \forall r \leq \tau. \quad (\text{B1})$$

Choosing any (infinite-dimensional) basis, every element of $\sum_{m,n=0}^{\infty} \frac{r^{m+n} e^{i(m-n)\phi}}{\sqrt{m!n!}} (\Psi - \Phi)[|m\rangle\langle n|]$ must equal 0, for any $r \leq \tau$. This can only be fulfilled if every element of $(\Psi - \Phi)[|m\rangle\langle n|]$ is identically 0, so $\|(\Psi - \Phi)[|re^{i\phi}\rangle\langle re^{i\phi}|_{\text{coh}}]\| = 0$ for all r (including $r > \tau$). This is also in line with what we expect from [5], since it is shown there that the quantum process matrix of a channel, Ψ , is completely determined by all of the (infinite) derivatives of $\|(\Psi - \Phi)[|re^{i\phi}\rangle\langle re^{i\phi}|_{\text{coh}}]\|$ assessed at the origin. Since they must all be the same for both Ψ and Φ over a finite region that includes the origin, the processes are identical everywhere.

We revisit the case of $\epsilon_0 > 0$ in Appendix I.

Appendix C: Gaussian channels

The output fidelity for Gaussian channels takes the form given in Eq. (23). By bounding x , y , and z individually, we can bound the output fidelity for any r . We have a constraint on the output distance for $r \leq \tau$, which translates into a lower bound on the fidelity via the Fuchs-van de Graaf. Specifically, for all $r \leq \tau$,

$$F\left[\mathcal{G}_1[|re^{i\phi}\rangle\langle re^{i\phi}|_{\text{coh}}], \mathcal{G}_2[|re^{i\phi}\rangle\langle re^{i\phi}|_{\text{coh}}]\right] \geq \frac{2 - \epsilon_0}{2}. \quad (\text{C1})$$

At $r = 0$, the output fidelity is x , so the lower bound on x follows directly. Now consider $r = \pm\tau$, for which we have

$$xe^{-y\tau^2 \mp z\tau} \geq \left(\frac{2 - \epsilon_0}{2}\right)^2. \quad (\text{C2})$$

If we want to maximise y and $|z|$, we should make x as large as possible, i.e., 1. Then, to bound y , we set $z = 0$ and get

$$e^{-y\tau^2} \geq \left(\frac{2 - \epsilon_0}{2}\right)^2, \quad (\text{C3})$$

and so recover our bound on y . Finally, we bound $|z|$ by comparing F^2 at $r = 0$ and at $r = \pm\tau$. Concavity can be confirmed by differentiating Eq. (25) twice with regard to r^2 .

A phase rotation of θ maps $|\alpha\rangle_{\text{coh}}$ to $|e^{i\theta}\alpha\rangle_{\text{coh}}$. The output fidelity between a target and a learned phase rotation, parametrised by θ_T and θ_L respectively, is $F_{\text{PR}}^2 = e^{-2|\alpha|^2(1-\cos(\theta_T-\theta_L))}$. If we are guaranteed that, for some τ and ϵ_0 , $\|(\Psi - \Phi)[|\tau e^{i\phi}\rangle\langle\tau e^{i\phi}|_{\text{coh}}]\| \leq \epsilon_0$, then $1 - \cos(\theta_T - \theta_L) \leq -\frac{\log[1-\frac{\epsilon_0}{2}]}{2\tau^2}$, so we recover Eq. (26). Note that we have used the tighter Fuchs-van de Graaf relation for pure states.

Applying single-mode squeezing to $|\alpha\rangle_{\text{coh}}$, the first and second moments become

$$V = \begin{pmatrix} e^{2s} & 0 \\ 0 & e^{-2s} \end{pmatrix}, \quad x = \begin{pmatrix} 2e^s \alpha_R \\ 2e^{-s} \alpha_I \end{pmatrix}, \quad (\text{C4})$$

so the output fidelity between a target and learned squeezing unitary is $F_{\text{sq}}^2 = \text{sech}(s_T - s_L) \exp[2|\alpha|^2(\text{sech}(s_T - s_L) - 1)]$. If we are again given $\|(\Psi - \Phi)[|\tau e^{i\phi}\rangle\langle\tau e^{i\phi}|_{\text{coh}}]\| \leq \epsilon_0$ for some τ , we get the condition $\text{sech}(s_T - s_L) \geq \frac{1}{2\tau^2} W_0[e^{2\tau^2} \tau^2 (2 - \epsilon_0)]$, where W_0 is the Lambert W function. The right hand side goes to 1 as $\epsilon_0 \rightarrow 0$, as expected. We therefore recover Eq. (27).

Appendix D: Out-of-distribution generalisation for classical states

From the convexity of the trace norm, we can write

$$\|(\Psi - \Phi)[\rho_{\text{class}}]\| \leq \int_0^\infty \epsilon(\epsilon_0, r^2) \int_0^{2\pi} P_{\text{class}}(r e^{i\phi}) r d\phi dr = \int_0^\infty \epsilon(\epsilon_0, r^2) p_{\text{class}}(r) dr, \quad (\text{D1})$$

where we have defined $p(r) = \int_0^{2\pi} P(r e^{i\phi}) r d\phi$. Using this definition, $\int_0^\infty p(r) dr = 1$ for any normalised P-representation, and our energy constraint takes the form $\int_0^\infty r^2 p(r) dr \leq \bar{n}$.

Now we apply Jensen's inequality for concave functions. The right hand side of Eq. (D1) can be expressed as the expectation value of $\epsilon(\epsilon_0, r^2)$ over the classical probability density function $p_{\text{class}}(r)$. For any valid probability density function

$$\mathbb{E}_{p_{\text{class}}}[\epsilon(\epsilon_0, r^2)] \leq \epsilon(\epsilon_0, \mathbb{E}_{p_{\text{class}}}[r^2]) \leq \epsilon(\epsilon_0, \mathbb{E}_{p_{\text{class}}}[\bar{n}]). \quad (\text{D2})$$

Note that since \bar{n} is the expectation value of r^2 and not of r , we only require concavity in r^2 .

Appendix E: Sufficiency of upper bounding μ

Recall that the quantity in Eq. (18) that we want to bound is $\mu\epsilon(\frac{\nu}{\mu})$, where $\epsilon(x)$ is concave in x and where we have temporarily dropped the dependence on ϵ_0 . Recall that μ and ν are defined by

$$\mu = 1 + 2\mathcal{N}, \quad \nu = (1 + \mathcal{N})\bar{n}_+ + \mathcal{N}\bar{n}_-. \quad (\text{E1})$$

The negativity of a state ρ is defined as the negative volume of the P-representation, i.e.,

$$\mathcal{N} = - \int_{P(\alpha)[\rho] < 0} P(\alpha)[\rho] d^2\alpha, \quad (\text{E2})$$

and \bar{n}_\pm are defined by

$$\bar{n}_+ = \frac{1}{1 + \mathcal{N}} \int_{P(\alpha) > 0} P(\alpha) |\alpha|^2 d^2\alpha, \quad \bar{n}_- = -\frac{1}{\mathcal{N}} \int_{P(\alpha) < 0} P(\alpha) |\alpha|^2 d^2\alpha. \quad (\text{E3})$$

Hence, μ and ν can be calculated as

$$\mu = \int |P(\alpha)| d^2\alpha, \quad \nu = \int |P(\alpha)| |\alpha|^2 d^2\alpha, \quad (\text{E4})$$

where we integrate over both the negative and the positive domains of the P-distribution, but take the absolute value.

At first glance, upper bounding $\mu\epsilon(\frac{\nu}{\mu})$ requires us to find both an upper and a lower bound on μ (and an upper bound on ν), since it is used both as a multiplicative factor and as the denominator, inside the function ϵ . However, by applying the concavity, we can show that it suffices to find an upper bound on μ .

Taking the partial derivative of $\mu\epsilon\left(\frac{\nu}{\mu}\right)$ with regard to μ , we get

$$\frac{\partial}{\partial\mu} \left[\mu\epsilon\left(\frac{\nu}{\mu}\right) \right] = \epsilon\left(\frac{\nu}{\mu}\right) - \frac{\nu}{\mu}\epsilon'\left(\frac{\nu}{\mu}\right), \quad (\text{E5})$$

where ϵ' is the partial derivative of ϵ with regard to μ . Then, recalling that $\epsilon'\left(\frac{\nu}{\mu}\right)$ is the gradient of ϵ at $\frac{\nu}{\mu}$ and applying the concavity of ϵ , we see that $\frac{\partial}{\partial\mu} \left[\mu\epsilon\left(\frac{\nu}{\mu}\right) \right] \geq 0$ for any (valid) value of μ . Thus, an overestimate of μ always results in an overestimate of $\mu\epsilon\left(\frac{\nu}{\mu}\right)$, and so it suffices to use an upper bound of μ , both inside and outside ϵ , when bounding $\mu\epsilon\left(\frac{\nu}{\mu}\right)$.

Appendix F: Bounding the output distance for $\sigma_{s,M}$

The P-representation, $P_{s,M}$, of $\sigma_{s,M}$ (the state obtained by first truncating ρ to a maximum photon number of $M-1$ and then convolving the resulting P-representation with a Gaussian function of width s^{-1}), can be written as

$$P_{s,M}(\alpha)[\rho] = P_{s,M}(re^{i\phi})[\rho] = \sum_{m,n=0}^{M-1} \langle m|\rho^{(M)}|n\rangle P_s(re^{i\phi})[|m\rangle\langle n|], \quad (\text{F1})$$

where $|m\rangle$ and $|n\rangle$ are Fock states. The contribution to $P_s(re^{i\phi})$ of the terms $|m\rangle\langle n|$ and $|n\rangle\langle m|$, where $m > n$, is ([49], Eq. 2.15)

$$\begin{aligned} P_s(re^{i\phi}) \left[\frac{1}{2}(e^{i\theta}|m\rangle\langle n| + e^{-i\theta}|n\rangle\langle m|) \right] &= P_{s,\theta}^{(m,n)}(re^{i\phi}) \\ &= \cos(\theta - (m-n)\phi) \frac{(-1)^n}{\pi} \sqrt{\frac{n!}{m!}} \frac{(1-s)^n}{s^{m+1}} e^{-\frac{1}{s}r^2} r^{m-n} L_n^{m-n} \left[\frac{r^2}{s(1-s)} \right], \end{aligned} \quad (\text{F2})$$

where L_x^y is a generalised Laguerre polynomial. We include θ for completeness, but will find it has no effect on our calculations and so will generally drop it from the subscript. For Fock states, $|m\rangle\langle m|$, we get Eq. (35). Eq. (35) has no angular dependence, whilst the angular component of Eq. (F2) is a cosine function of period $\frac{2\pi}{m-n}$. We will upper bound μ and ν by finding and summing the contributions from each term $P_s^{(m,n)}$; this is just an upper bound and is not tight unless the different contributions to the total P-representations never cancel each other out (which is not generally the case). Noting that the P-representation contributions of the on and off-diagonal elements of $\rho^{(M)}$ have different properties (despite one being a special case of the other), it is helpful to separate their contributions to μ and ν .

Starting with the off-diagonals, and using Eq. (F2), the exact contributions to μ and ν are

$$\mu[P_s^{(m,n)}] = \frac{1}{\pi} \frac{(1-s)^n}{s^{m+1}} \sqrt{\frac{n!}{m!}} \int_0^{2\pi} |\cos(\theta - (m-n)\phi)| d\phi \int_0^\infty e^{-\frac{1}{s}r^2} r^{m-n+1} \left| L_n^{m-n} \left[\frac{r^2}{s(1-s)} \right] \right| dr, \quad (\text{F3})$$

$$\nu[P_s^{(m,n)}] = \frac{1}{\pi} \frac{(1-s)^n}{s^{m+1}} \sqrt{\frac{n!}{m!}} \int_0^{2\pi} |\cos(\theta - (m-n)\phi)| d\phi \int_0^\infty e^{-\frac{1}{s}r^2} r^{m-n+3} \left| L_n^{m-n} \left[\frac{r^2}{s(1-s)} \right] \right| dr. \quad (\text{F4})$$

The integral over ϕ is always equal to 4. Then, applying a bound (by Szegő) on the magnitude of Laguerre polynomials,

$$\mu[P_s^{(m,n)}] \leq \frac{4}{\pi} \frac{(1-s)^n}{s^{m+1}} \frac{(m-n+1)_n}{\sqrt{m!n!}} \int_0^\infty r^{m-n+1} e^{\frac{r^2}{s} \left(\frac{1}{2(1-s)} - 1 \right)} dr, \quad (\text{F5})$$

$$\nu[P_s^{(m,n)}] \leq \frac{4}{\pi} \frac{(1-s)^n}{s^{m+1}} \frac{(m-n+1)_n}{\sqrt{m!n!}} \int_0^\infty r^{m-n+3} e^{\frac{r^2}{s} \left(\frac{1}{2(1-s)} - 1 \right)} dr, \quad (\text{F6})$$

where $(x)_n$ is the Pochhammer symbol. These integrals converge for $s < \frac{1}{2}$. Evaluating them, we get

$$\mu[P_s^{(m,n)}] \leq \frac{2}{\pi} \frac{(1-s)^n}{s^{m+1}} \frac{(m-n+1)_n}{\sqrt{m!n!}} \left(\frac{2s(1-s)}{1-2s} \right)^{1+\frac{m-n}{2}} \Gamma \left[1 + \frac{m-n}{2} \right], \quad (\text{F7})$$

$$\nu[P_s^{(m,n)}] \leq \frac{2}{\pi} \frac{(1-s)^n}{s^{m+1}} \frac{(m-n+1)_n}{\sqrt{m!n!}} \left(\frac{2s(1-s)}{1-2s} \right)^{2+\frac{m-n}{2}} \Gamma \left[2 + \frac{m-n}{2} \right]. \quad (\text{F8})$$

After some simplification, we end up with the inequalities:

$$\mu[P_s^{(m,n)}] \leq \frac{2^{2+\frac{m-n}{2}}(1-s)^{1+\frac{m+n}{2}}(m-n+1)_n}{\pi s^{\frac{m+n}{2}}(1-2s)^{1+\frac{m-n}{2}}\sqrt{m!n!}}\Gamma\left[1+\frac{m-n}{2}\right], \quad (\text{F9})$$

$$\nu[P_s^{(m,n)}] \leq \frac{2^{3+\frac{m-n}{2}}(1-s)^{2+\frac{m+n}{2}}(m-n+1)_n}{\pi s^{\frac{m+n}{2}-1}(1-2s)^{2+\frac{m-n}{2}}\sqrt{m!n!}}\Gamma\left[2+\frac{m-n}{2}\right]. \quad (\text{F10})$$

We now use Eq. (35) to find the contributions from the on-diagonals:

$$\mu[P_s^{(m,m)}] = \frac{1}{\pi} \frac{(1-s)^m}{s^{m+1}} \int_0^{2\pi} 1d\phi \int_0^\infty e^{-\frac{1}{s}r^2} r \left| L_m \left[\frac{r^2}{s(1-s)} \right] \right| dr, \quad (\text{F11})$$

$$\nu[P_s^{(m,m)}] = \frac{1}{\pi} \frac{(1-s)^m}{s^{m+1}} \int_0^{2\pi} 1d\phi \int_0^\infty e^{-\frac{1}{s}r^2} r^3 \left| L_m \left[\frac{r^2}{s(1-s)} \right] \right| dr. \quad (\text{F12})$$

Again using the bound on the magnitude of the Laguerre polynomials,

$$\mu[P_s^{(m,m)}] \leq 2 \frac{(1-s)^m}{s^{m+1}} \int_0^\infty r e^{\frac{r^2}{s}(\frac{1}{2(1-s)}-1)} dr = 2 \frac{(1-s)^{m+1}}{s^m(1-2s)}, \quad (\text{F13})$$

$$\nu[P_s^{(m,m)}] \leq 2 \frac{(1-s)^m}{s^{m+1}} \int_0^\infty r^3 e^{\frac{r^2}{s}(\frac{1}{2(1-s)}-1)} dr = 4 \frac{(1-s)^{m+2}}{s^{m-1}(1-2s)^2}. \quad (\text{F14})$$

We can therefore upper bound $\mu[P_{s,M}] = \mu_{s,M}$, based on the number state decomposition of ρ , as

$$\mu_{s,M}^{(\text{UB})} = \sum_{m,n=0}^{M-1} |\langle m|\rho|n\rangle| \mu_{s,m,n} \geq \mu_{s,M}, \quad (\text{F15})$$

$$\mu_{s,m,m} = \frac{2(1-s)^{m+1}}{s^m(1-2s)}, \quad \mu_{s,m,n \neq m} = \frac{2^{2+\frac{|m-n|}{2}}(1-s)^{1+\frac{m+n}{2}}(|m-n|+1)_{\min[m,n]}}{\pi s^{\frac{m+n}{2}}(1-2s)^{1+\frac{|m-n|}{2}}\sqrt{m!n!}}\Gamma\left[1+\frac{|m-n|}{2}\right]. \quad (\text{F16})$$

By comparing Eqs. (F9) and (F10) and Eqs. (F13) and (F14), we see that, in both the on and off-diagonal cases, the ratio between (the upper bounds on) the contributions to ν and μ can be expressed (for $m \geq n$) as

$$\frac{\nu^{(\text{UB})}[P_s^{(m,n)}]}{\mu^{(\text{UB})}[P_s^{(m,n)}]} = \frac{s(1-s)}{1-2s}(2+m-n). \quad (\text{F17})$$

We now have two options: we can explicitly write upper bounds on μ and ν , by combining Eqs. (F9), (F10), (F13), and (F14) with a number state description of ρ or we can upper bound the ratio between $\nu^{(\text{UB})}$ and $\mu^{(\text{UB})}$ (though perhaps loosely) as

$$\frac{\nu^{(\text{UB})}[P_{s,M}]}{\mu^{(\text{UB})}[P_{s,M}]} \leq \frac{s(1-s)}{1-2s}(M+1). \quad (\text{F18})$$

Eq. (F18) is less than $\sim \frac{M}{2}$ times the true bound and ϵ is concave, so we choose this method. We therefore arrive at Eq. (19).

Appendix G: Bounding the output distance over all states

To upper bound $\mu^{(\text{UB})}$ over all states ρ , we use the fact ρ is a positive semi-definite matrix, and hence:

$$|\langle m|\rho|n\rangle| \leq \frac{\langle m|\rho|m\rangle + \langle n|\rho|n\rangle}{2}. \quad (\text{G1})$$

Upper bounding the upper bound on μ from Eq. (F15), we get

$$\mu_{s,M}^{(\text{UB})} \leq \sum_{m,n=0}^{M-1} \frac{\langle m|\rho|m\rangle + \langle n|\rho|n\rangle}{2} \mu_{s,m,n} = \sum_{m=0}^{M-1} \langle m|\rho|m\rangle \sum_{n=0}^{M-1} \mu_{s,m,n} \leq \max_m \left[\sum_{n=0}^{M-1} \mu_{s,m,n} \right]. \quad (\text{G2})$$

For small s , we will show that this maximum is achieved by setting $m = M - 1$. We must note that we are taking an upper bound on an upper bound here, so should expect the resulting bound on μ to be very loose. However, this is also to be expected, as our goal is to make an extremely general statement that holds even without having any description of the input state at all, other than knowing its average photon number. We could improve this bound somewhat by using the average photon number (i.e., by accounting for the fact $\sum_m \langle m | \rho | m \rangle = \bar{n}$), but this would result in more complicated expressions.

We can upper bound the row sum $\sum_{n=0}^{M-1} \mu_{s,m,n}$ by bounding the ratio between neighbouring terms. We start by calculating

$$\frac{\mu_{s,m,n}}{\mu_{s,m,n-1}} = \sqrt{\frac{(1-s)(1-2s)}{2s}} \frac{m-n+1}{\sqrt{n}} \frac{\Gamma[\frac{m-n+2}{2}]}{\Gamma[\frac{m-n+3}{2}]} > \sqrt{\frac{(1-s)(1-2s)}{s}} \frac{m-n+1}{\sqrt{n(m-n+3)}} \quad \text{for } m > n, \quad (\text{G3})$$

where we bound the ratio between gamma functions using Gautschi's inequality. Similarly,

$$\frac{\mu_{s,m,n+1}}{\mu_{s,m,n}} = \sqrt{\frac{2(1-s)}{s(1-2s)}} \frac{\sqrt{n+1}}{n-m+1} \frac{\Gamma[\frac{n-m+3}{2}]}{\Gamma[\frac{n-m+2}{2}]} > \sqrt{\frac{1-s}{s(1-2s)}} \sqrt{\frac{n+1}{n-m+1}} \quad \text{for } m < n. \quad (\text{G4})$$

Next, we calculate

$$\frac{\mu_{s,m,m}}{\mu_{s,m,m-1}} = \sqrt{\frac{\pi}{2}} \sqrt{\frac{(1-s)(1-2s)}{sm}}, \quad \frac{\mu_{s,m,m+1}}{\mu_{s,m,m}} = \sqrt{\frac{2}{\pi}} \sqrt{\frac{(1-s)(m+1)}{s(1-2s)}}, \quad (\text{G5})$$

where we have used $\Gamma[\frac{3}{2}] = \frac{\sqrt{\pi}}{2}$. Upper and lower bounding the n -dependent terms (for $m \neq 0$),

$$\frac{\mu_{s,m,n}}{\mu_{s,m,n-1}} > \sqrt{\frac{(1-s)(1-2s)}{sm}} \quad \text{for } m \geq n, \quad \frac{\mu_{s,m,n+1}}{\mu_{s,m,n}} > \sqrt{\frac{1-s}{s(1-2s)}} \quad \text{for } m \leq n. \quad (\text{G6})$$

From Eq. (G6), we can see that, so long as s decreases at least with M^{-1} (more specifically, as long as $\frac{(1-s)(1-2s)}{s(M-1)} > 1$), each $\mu_{s,m,n-1} < \mu_{s,m,n}$ (for both $m \geq n$ and $m < n$). Since $\mu_{s,m,n} = \mu_{s,n,m}$, this means $\sum_{n=0}^{M-1} \mu_{s,m-1,n} < \sum_{n=0}^{M-1} \mu_{s,m,n}$. Hence, the $m = M - 1$ row has the largest row sum, and thus (using Eq. (F16))

$$\mu_{s,M}^{(\text{UB})} \leq \sum_{n=0}^{M-1} \mu_{s,M-1,n} < \mu_{s,M-1,M-1} \sum_{k=0}^{M-1} \left(\frac{s(M-1)}{(1-s)(1-2s)} \right)^{\frac{k}{2}} < \frac{2(1-s)M}{s^{M-1}(1-2s)}, \quad (\text{G7})$$

where we could have used the formula for the sum of a geometric sequence to obtain a slightly tighter bound.

Substituting Eq. (G7) into Eq. (20)

$$\|(\Psi - \Phi)[\rho]\| \leq \left(1 - \frac{\bar{n}}{M}\right) \left(\frac{2(1-s)M}{s^{M-1}(1-2s)} \epsilon \left(\epsilon_0, \frac{s(1-s)(M+1)}{1-2s} \right) + 4\sqrt{s(1+2\bar{n})} \right) + \frac{2\bar{n}}{M}. \quad (\text{G8})$$

Finally, we pick a particular relationship between s and M , but note that this is not a unique, nor even necessarily optimal (in terms of giving the tightest possible bound), choice. Specifically, we choose $s = \frac{1}{\kappa(M+3)}$, for some $\kappa > 1$. $M+3$ is used instead of M to ensure the argument to ϵ is upper bounded by $\frac{s(1-s)(M+1)}{1-2s} < \frac{1}{\kappa}$ for all $\kappa > 1$. Then Eq. (G8) is bounded by Eq. (1) from the main text.

Appendix H: Distance of $\sigma_{s,M}$ from $\rho^{(M)}$

Our goal is to determine how far each state in our parametrised sequence, $\{\sigma_{s,M}\}$, is from the truncated state, $\rho^{(M)}$. Recall that each state $\sigma_{s,M}$ is obtained from ρ by first truncating it to an M -dimensional representation, $\rho^{(M)}$, and then convolving the P-representation of the resulting state, $P_M(\alpha)$, with $\frac{1}{s\pi} e^{-\frac{1}{s}|\alpha|^2}$ (equivalently, applying channel \mathcal{C}_s), to obtain state $\sigma_{s,M}$, with P-representation $P_{s,M}(\alpha)$. It is clear that as $M \rightarrow \infty$ and $s \rightarrow 0$, $\sigma_{s,M}$ converges to ρ , but we are interested in the rate of convergence.

We will bound δ_s by calculating the fidelity between $\rho^{(M)}$ and $\sigma_{s,M}$ and applying a Fuchs-van de Graaf inequality. The overlap between the states, $\text{Tr}[\rho^{(M)}\sigma_{s,M}]$ is given by

$$\text{Tr}[\rho^{(M)}\sigma_{s,M}] = \pi \int P_s(\alpha)[\rho^{(M)}]Q(\alpha)[\rho^{(M)}]d^2\alpha = \pi \int \left(\frac{1}{s\pi} e^{-\frac{1}{s}|\alpha|^2} \star P(\alpha)[\rho^{(M)}] \right) \left(\frac{1}{\pi} e^{-|\alpha|^2} \star P(\alpha)[\rho^{(M)}] \right) d^2\alpha, \quad (\text{H1})$$

where $Q(\alpha)$ is the Husimi Q-representation. Since $F(A, B)^2 \geq \text{Tr}[AB]$, we can use this overlap to bound the fidelity (sometimes defined as the square of the quantity that we call fidelity here). However, some care is required here, since our lower bound on the squared fidelity based on the overlap is not tight, and does not converge to 1 as $s \rightarrow 0$ unless the state is pure.

First, we assess $\text{Tr}[|\psi\rangle\langle\psi| \mathcal{C}_s[|\psi\rangle\langle\psi|]]$ for an arbitrary (pure) state $|\psi\rangle$ (lying in the Hilbert space of $\rho^{(M)}$). We can express $|\psi\rangle$ as $\sum_{m=0}^{M-1} a_m |m\rangle$ for some complex parameters $\{a_m\}$ such that $\sum_{m=0}^{M-1} a_m a_m^* = 1$. The P-representation of $\mathcal{C}[|\psi\rangle\langle\psi|]$ is

$$P_s[|\psi\rangle\langle\psi|] = \sum_{m,n=0}^{M-1} |a_m a_n^*| P_{s,\theta(m,n)}^{(m,n)}, \quad \theta(m,n) = \arg[a_{\max[m,n]} a_{\min[m,n]}^*], \quad (\text{H2})$$

where the expressions for $P_s^{(m,n)}$ are given by Eqs. (F2) and (35) and where we have again included the subscript θ for completeness. The linearity of the trace means we can decompose $\text{Tr}[|\psi\rangle\langle\psi| \mathcal{C}_s[|\psi\rangle\langle\psi|]]$ into a sum of contributions:

$$\begin{aligned} \text{Tr}[|\psi\rangle\langle\psi| \mathcal{C}_s[|\psi\rangle\langle\psi|]] &= \pi \int P_s(\alpha)[|\psi\rangle\langle\psi|] Q(\alpha)[|\psi\rangle\langle\psi|] d^2\alpha \\ &= \sum_{m_1, n_1=0} \sum_{m_2, n_2=0} |a_{m_1} a_{n_1}^* a_{m_2} a_{n_2}^*| \gamma_s(m_1, n_1, \theta_1, m_2, n_2, \theta_2), \end{aligned} \quad (\text{H3})$$

where each contribution $\gamma_s(m_1, n_1, \theta_1, m_2, n_2, \theta_2)$ is defined by

$$\gamma_s(m_1, n_1, \theta_1, m_2, n_2, \theta_2) = \pi \int_0^\infty \int_0^{2\pi} P_{s,\theta_1}^{(m_1, n_1)}(re^{i\phi}) Q_{\theta_2}^{(m_2, n_2)}(re^{i\phi}) r d\phi dr, \quad (\text{H4})$$

$$Q_\theta^{(m,n)}(re^{i\phi}) = \lim_{s \rightarrow 1} P_{s,\theta}^{(m,n)}(re^{i\phi}) = \cos(\theta - (m-n)\phi) \frac{e^{-r^2} r^{m+n}}{\pi \sqrt{m!n!}}, \quad (\text{H5})$$

$$Q^{(m,m)}(re^{i\phi}) = \lim_{s \rightarrow 1} P_s^{(m,m)}(re^{i\phi}) = \frac{e^{-r^2} r^{2m}}{\pi m!}. \quad (\text{H6})$$

From the angular dependence of the P and Q-representations, it is immediate that $\gamma_s(m_1, n_1, \theta_1, m_2, n_2, \theta_2)$ is only non-zero if $|m_1 - n_1| = |m_2 - n_2|$. This is because, for $|m_1 - n_1| \neq |m_2 - n_2|$,

$$\int_0^{2\pi} \cos(\theta_1 - (m_1 - n_1)\phi) \cos(\theta_2 - (m_2 - n_2)\phi) d\phi = 0. \quad (\text{H7})$$

Note too that $\gamma_s(m_1, n_1, \theta_1, m_2, n_2, \theta_2)$ is symmetric under swapping m and n , so we can set $m \geq n$.

Starting by looking at the off-diagonals, and setting $\Delta = m - n$ and $m > n$,

$$\begin{aligned} \gamma_s(m_1, m_1 - \Delta, \theta_1, m_2, m_2 - \Delta, \theta_2) &= \sqrt{\frac{(m_1 - \Delta)!}{m_1! m_2! (m_2 - \Delta)!}} \frac{(s-1)^{m_1 - \Delta}}{\pi s^{m_1 + 1}} \int_0^{2\pi} \cos(\theta_1 - \Delta\phi) \cos(\theta_2 - \Delta\phi) d\phi \\ &\quad \times \int_0^\infty e^{-\frac{1+s}{s} r^2} r^{2m_2 + 1} L_{m_1 - \Delta}^\Delta \left[\frac{r^2}{s(1-s)} \right] dr. \end{aligned} \quad (\text{H8})$$

Then, by carrying out the integration over ϕ and explicitly expanding the Laguerre polynomial

$$\begin{aligned} \gamma_s(m_1, m_1 - \Delta, \theta_1, m_2, m_2 - \Delta, \theta_2) &= \cos(\theta_1 - \theta_2) \sqrt{\frac{(m_1 - \Delta)!}{m_1! m_2! (m_2 - \Delta)!}} \frac{(s-1)^{m_1 - \Delta}}{s^{m_1 + 1}} \\ &\quad \times \sum_{i=0}^{m_1 - \Delta} \frac{(-1)^i}{s^i (1-s)^i i!} \binom{m_1}{\Delta + i} \int_0^\infty e^{-\frac{1+s}{s} r^2} r^{2(m_2 + i) + 1} dr. \end{aligned} \quad (\text{H9})$$

Next, we calculate that for any non-negative integer x ,

$$\int_0^\infty e^{-\frac{1+s}{s} r^2} r^{2x+1} dr = \frac{x!}{2} \left(\frac{s}{1+s} \right)^{1+x}, \quad (\text{H10})$$

where, per convention, $0! = 1$. Using Eq. (H10), we get

$$\begin{aligned} \gamma_s(m_1, m_1 - \Delta, \theta_1, m_2, m_2 - \Delta, \theta_2) &= \cos(\theta_1 - \theta_2) \frac{s^{m_2 - m_1}}{2} \sqrt{\frac{(m_1 - \Delta)!}{m_1! m_2! (m_2 - \Delta)!}} \frac{(s-1)^{m_1 - \Delta}}{(1+s)^{m_2 + 1}} \sum_{i=0}^{m_1 - \Delta} \frac{(m_2 + i)!}{(s^2 - 1)^i i!} \binom{m_1}{\Delta + i} \\ &= \cos(\theta_1 - \theta_2) \frac{s^{m_2 - m_1}}{2} \sqrt{\binom{m_1}{\Delta} \binom{m_2}{\Delta}} \frac{{}_2F_1(\Delta - m_1, m_2 + 1, \Delta + 1, (1-s^2)^{-1})}{(1+s)^{m_2 + 1} (s-1)^{\Delta - m_1}}, \end{aligned} \quad (\text{H11})$$

where ${}_2F_1(a, b, c, z)$ is the hypergeometric function. Applying the Pfaff transformation rule for hypergeometric functions,

$$\gamma_s(m_1, m_1 - \Delta, \theta_1, m_2, m_2 - \Delta, \theta_2) = \frac{\cos(\theta_1 - \theta_2)}{2} \sqrt{\binom{m_1}{\Delta} \binom{m_2}{\Delta}} \frac{{}_2F_1(\Delta - m_1, \Delta - m_2, \Delta + 1, s^{-2})}{s^{2\Delta - m_1 - m_2} (1 + s)^{m_1 + m_2 + 1 - \Delta}}. \quad (\text{H12})$$

This rearrangement is useful because it highlights the fact that γ_s is symmetric under swapping m_1 and m_2 (and θ_1 and θ_2), but also because ${}_2F_1(\Delta - m_1, \Delta - m_2, \Delta + 1, s^{-2})$ can be expressed as a sum over only positive terms (rather than a sum of terms with alternating signs). Since γ_s is symmetric, we set $m_1 \leq m_2$. Then, since $\Delta - m_1 = -n_1$ and $\Delta - m_2 = -n_2$ are both negative (we will substitute back and forth between m and n depending on what is easiest),

$$\begin{aligned} s^{m_1 + m_2 - 2\Delta} {}_2F_1(\Delta - m_1, \Delta - m_2, \Delta + 1, s^{-2}) &= s^{n_1 + n_2} \sum_{k=0}^{n_1} (-1)^k \binom{n_1}{k} \frac{(-n_2)_k}{(\Delta + 1)_k} s^{-2k} \\ &= s^{n_2 - n_1} \sum_{k=0}^{n_1} \binom{n_1}{k} \frac{n_2!}{(n_2 - k)!} \frac{\Delta!}{(\Delta + 1)!} s^{2(n_1 - k)}. \end{aligned} \quad (\text{H13})$$

We define the polynomial

$$G[m_1, m_2, \Delta, s] = \sum_{k=0}^{n_1} \binom{n_1}{k} \frac{n_2!}{(n_2 - k)!} \frac{\Delta!}{(\Delta + k)!} s^{2(n_1 - k)}, \quad (\text{H14})$$

where we assume $m_2 \geq m_1 \geq \Delta$. Crucially, this is a polynomial in s that only has positive coefficients, so we are guaranteed that it will evaluate to a finite, positive value for any value of s . Finally, we can rewrite Eq. (H12) as

$$\gamma_s(m_1, m_1 - \Delta, \theta_1, m_2, m_2 - \Delta, \theta_2) = \frac{\cos(\theta_1 - \theta_2)}{2} \sqrt{\binom{m_1}{\Delta} \binom{m_2}{\Delta}} \frac{s^{m_2 - m_1} G[m_1, m_2, \Delta, s]}{(1 + s)^{m_1 + m_2 + 1 - \Delta}}. \quad (\text{H15})$$

For on-diagonals ($m = n$), we have

$$\begin{aligned} \gamma_s(m_1, m_1, m_2, m_2) &= \frac{1}{m_2!} \frac{(s-1)^{m_1}}{\pi s^{m_1+1}} \int_0^{2\pi} 1 d\phi \int_0^\infty e^{-\frac{1+s}{s} r^2} r^{2m_2+1} L_{m_1} \left[\frac{r^2}{s(1-s)} \right] dr \\ &= \frac{2}{m_2!} \frac{(s-1)^{m_1}}{s^{m_1+1}} \sum_{i=0}^{m_1} \binom{m_1}{i} \frac{(-1)^i}{s^i (1-s)^i i!} \int_0^\infty e^{-\frac{1+s}{s} r^2} r^{2(m_2+i)+1} dr \\ &= \frac{s^{m_2 - m_1}}{m_2!} \frac{(s-1)^{m_1}}{(1+s)^{m_2+1}} \sum_{i=0}^{m_1} \binom{m_1}{i} \frac{(m_2+i)!}{(s^2-1)^i i!} \\ &= s^{m_2 - m_1} \frac{(s-1)^{m_1}}{(1+s)^{m_2+1}} {}_2F_1(-m_1, m_2+1, 1, (1-s^2)^{-1}) \\ &= s^{m_1 + m_2} \frac{{}_2F_1(-m_1, -m_2, 1, s^{-2})}{(1+s)^{m_1 + m_2 + 1}}, \end{aligned} \quad (\text{H16})$$

where the only difference from the off-diagonal case is in the prefactor, coming from the integration of the angular part. We have dropped the θ -dependence because, per Eq. (H2), for $m = n$, $\theta = \arg[a_m a_m^*] = 0$. Again, the expression is symmetric under interchange of m_1 and m_2 , so we again set $m_2 \geq m_1$. Then,

$$\gamma_s(m_1, m_1, m_2, m_2) = s^{m_2 - m_1} \sum_{k=0}^{m_1} \binom{m_1}{k} \frac{m_2!}{(m_2 - k)! k!} s^{2(m_1 - k)} = \frac{s^{m_2 - m_1} G[m_1, m_2, 0, s]}{(1 + s)^{m_1 + m_2 + 1}}. \quad (\text{H17})$$

Recall that we are only interested in the fidelity for small s . We will therefore construct a small- s approximation of the squared fidelity. From Eqs. (H15) and (H17), we can see that the gamma functions go to 0 as $s \rightarrow 0$ except in the case of $m_1 = m_2$, due to the prefactor of $s^{m_2 - m_1}$. For $m_1 = m_2$, Eqs. (H15) and (H17) become

$$\gamma_s(m, n, \theta, m, n, \theta) = \frac{1}{2} \binom{m}{n} \frac{G[m, m, m - n, s]}{(1 + s)^{m + n + 1}}, \quad (\text{H18})$$

$$\gamma_s(m, m, m, m) = \frac{G[m, m, 0, s]}{(1 + s)^{2m + 1}}. \quad (\text{H19})$$

From Eq. (H14), we can see that only the $k = n_1$ term survives as $s \rightarrow 0$, so Eqs.(H18) and (H19) go to $\frac{1}{2}$ and 1 respectively as $s \rightarrow 0$. Assessing Eq. (H3) for $s = 0$ (and again dropping unnecessary θ -dependence), we therefore get

$$\text{Tr}[|\psi\rangle\langle\psi| \mathcal{C}_0[|\psi\rangle\langle\psi|]] = \sum_{m=0} |a_m^4| \gamma_0(m, m, m, m) + 2 \sum_{\substack{m, n=0, \\ m \neq n}} |a_m^2 a_n^2| \gamma_0(m, n, m, n) = \sum_{m, n=0} |a_m^2 a_n^2| = 1, \quad (\text{H20})$$

where the factor of 2 comes from summing both $\gamma_0(m, n, m, n)$ and $\gamma_0(m, n, n, m)$.

To lower bound the fidelity for non-zero (but small) s , we take the lowest ordered terms of $\gamma_s(m, m, m, m)$ and $\gamma_s(m, n, m, n)$, i.e., we take the s^0 terms of Eqs. (H18) and (H19) and neglect all other terms. This is valid because, as we will now show, the sum over all terms of the form $\gamma_s(m, n, m + q, n + q)$ (for $q > 0$) is positive. I.e.,

$$\sum_{q=1}^{M-2} \sum_{m, n=0}^{M-1-q} (2 - \delta_{\text{kron}}(m, n)) |a_{m+q} a_{n+q} a_m a_n| \gamma_s(m, n, \theta_1, m + q, n + q, \theta_2) \geq 0, \quad (\text{H21})$$

where δ_{kron} is the Kronecker delta and the prefactor of $(2 - \delta_{\text{kron}}(m, n))$ is so that we count both $\gamma_s(m, n, m + q, n + q)$ and $\gamma_s(n, m, m + q, n + q)$ for $m \neq n$. For completeness, we should also sum over $\gamma_s(m + q, n + q, m, n)$ and $\gamma_s(m + q, n + q, n, m)$, but since this only results in a prefactor of 2 on all terms, we can neglect this. We rewrite Eq. (H15) (for $q > 0$ and $m \neq n$) as

$$\begin{aligned} \gamma_s(m, n, \theta_1, m + q, n + q, \theta_2) &= \frac{\cos(\theta_1 - \theta_2)}{2} \frac{\sqrt{m!n!(m+q)!(n+q)!}}{(1+s)^{m+n+q+1}} \sum_{j=0}^{\min[m,n]} \frac{s^{q+2j}}{j!(q+j)!(n-j)!(m-j)!} \\ &= \frac{1}{4|a_{m+q} a_{n+q} a_m a_n|} \sum_{j=0}^{\min[m,n]} \psi_{q,j,m} \psi_{q,j,n}^* + \psi_{q,j,m}^* \psi_{q,j,n}, \end{aligned} \quad (\text{H22})$$

where we define

$$\psi_{q,j,r} = \frac{a_r a_{r+q}^* s^{j+\frac{q}{2}} \sqrt{r!(r+q)!}}{(1+s)^{r+\frac{q+1}{2}} (r+q)! \sqrt{j!(q+j)!}} \quad (\text{H23})$$

and we use the fact that

$$a_m a_{m+q}^* a_n^* a_{n+q} + a_m^* a_{m+q} a_n a_{n+q}^* = 2|a_{m+q} a_{n+q} a_m a_n| \cos(\arg[a_m a_n^*] - \arg[a_{m+q} a_{n+q}^*]). \quad (\text{H24})$$

Similarly, Eq. (H17) becomes

$$\gamma_s(m, m, m + q, m + q) = \frac{1}{|a_{m+q}^2 a_m^2|} \sum_{j=0}^m \psi_{q,j,m} \psi_{q,j,m}^* \quad (\text{H25})$$

Thus, the condition from Eq. (H21), which we want to prove, becomes

$$\sum_{q=1}^{M-2} \sum_{m, n=0}^{M-1-q} \sum_{j=0}^{\min[m,n]} \psi_{q,j,m} \psi_{q,j,n}^* = \sum_{q=1}^{M-2} \sum_{j=0}^{M-1-q} \sum_{m, n=j}^{M-1-q} \psi_{q,j,m} \psi_{q,j,n}^* \geq 0. \quad (\text{H26})$$

Defining $\psi_{q,j}$ as the 1 by $M - j - q$ vector with entries $\psi_{q,j,r}$ for r ranging from j to $M - 1 - q$, we note that the left hand side of Eq. (H26) is the sum over q and j of the sum of all entries of the matrices $\psi_{q,j} \psi_{q,j}^\dagger$. Summing all entries of a positive semi-definite matrix gives a number that is ≥ 0 , and since $\psi_{q,j}^\dagger \psi_{q,j} \geq 0$, $\psi_{q,j} \psi_{q,j}^\dagger$ is positive semi-definite.

Hence, we can validly lower bound the fidelity by summing only the s^0 terms in Eqs. (H18) and (H19). Specifically, we write

$$\text{Tr}[|\psi\rangle\langle\psi| \mathcal{C}_s[|\psi\rangle\langle\psi|]] \geq \sum_{m, n=0}^{M-1} \frac{|a_m^2 a_n^2|}{(1+s)^{m+n+1}}, \quad (\text{H27})$$

where we only use the first term in $G[m, m, n, 0]$. This is a convex function in s , so for pure states, we can write

$$F^2(|\psi\rangle\langle\psi|, \mathcal{C}_s[|\psi\rangle\langle\psi|]) \geq 1 - s \sum_{m, n=0}^{M-1} |a_m^2 a_n^2| (m + n + 1) = 1 - s \left(1 + 2 \sum_{m=0}^{M-1} |a_m^2| m \right), \quad (\text{H28})$$

where we have lower bounded it using the first order Taylor expansion around $s = 0$. Using the definition of the average energy

$$F^2(|\psi\rangle\langle\psi|, \mathcal{C}_s[|\psi\rangle\langle\psi|]) \geq 1 - s(1 + 2\bar{n}(|\psi\rangle\langle\psi|)), \quad (\text{H29})$$

and from the Fuchs-van de Graaf relations,

$$\delta_s(|\psi\rangle\langle\psi|) \leq 2\sqrt{s(1 + 2\bar{n}(|\psi\rangle\langle\psi|))}. \quad (\text{H30})$$

Finally, using the convexity of the trace norm and Jensen's inequality, we arrive at Eq. (16) from the main text.

Appendix I: Out-of-distribution generalisation for coherent states when $\epsilon_0 > 0$

We now use some of the techniques from the previous appendices to revisit out-of-distribution generalisation for coherent states. The aim now is to explicitly show that we can always (i.e., regardless of the class of the target channel) construct a concave function $\epsilon(\epsilon_0, r^2)$ that bounds the output distance for coherent states and that has the properties listed in Theorem 2.

Recall that coherent states have the number state decomposition

$$|re^{i\phi}\rangle\langle re^{i\phi}|_{\text{coh}} = e^{-r^2} \sum_{m,n=0}^{\infty} \frac{r^{m+n} e^{i(m-n)\phi}}{\sqrt{m!n!}} |m\rangle\langle n|. \quad (\text{I1})$$

We use the same method as in Section IV B, replacing $|re^{i\phi}\rangle\langle re^{i\phi}|_{\text{coh}}$ with $\mathcal{C}_s(|re^{i\phi}\rangle\langle re^{i\phi}|_{\text{coh}})$. Per Eq. (16), $|re^{i\phi}\rangle\langle re^{i\phi}|_{\text{coh}}$ has a distance from $\mathcal{C}_s(|re^{i\phi}\rangle\langle re^{i\phi}|_{\text{coh}})$ of no more than $2\sqrt{s(1 + 2r^2)}$. We then upper bound $\|(\Psi - \Phi)[\mathcal{C}_s(|re^{i\phi}\rangle\langle re^{i\phi}|_{\text{coh}})]\|$ by bounding $\|(\Psi - \Phi)[\mathcal{C}_s(|m\rangle\langle m|)]\|$ and $\|(\Psi - \Phi)[\frac{1}{2}\mathcal{C}_s(e^{i\theta}|m\rangle\langle n| + e^{-i\theta}|n\rangle\langle m|)]\|$ for every m, n , and θ .

Note that we have previously upper bounded these same quantities (in Section VII B and Appendix F), however here our starting point is different. Previously, we assumed we had a known, concave function $\epsilon(\epsilon_0, r^2)$, but now finding such a function is the goal. Instead, we only assume that $\|(\Psi - \Phi)[|re^{i\phi}\rangle\langle re^{i\phi}|_{\text{coh}}]\| \leq \epsilon_0$ for $r^2 \leq \tau^2$. Then, we can apply the step function (ϵ_{step} from Eq. (6)) that assigns ϵ_0 for $r \leq \tau$ and 2 for $r > \tau$.

Recall that the P-representation of $|m\rangle\langle m|$ is given by Eq. (35). $\|(\Psi - \Phi)[\mathcal{C}_s(|m\rangle\langle m|)]\|$ can therefore be upper bounded by

$$\|(\Psi - \Phi)[\mathcal{C}_s(|m\rangle\langle m|)]\| \leq \epsilon_0 \mu_\tau [P_s^{(m,m)}] + 2 \left(\mu [P_s^{(m,m)}] - \mu_\tau [P_s^{(m,m)}] \right), \quad (\text{I2})$$

$$\mu_\tau [P_s^{(m,m)}] = \int_0^{2\pi} \int_0^\tau |P_s^{(m,m)}(re^{i\phi})| r d\phi dr, \quad \mu [P_s^{(m,m)}] = \int_0^{2\pi} \int_0^\infty |P_s^{(m,m)}(re^{i\phi})| r d\phi dr, \quad (\text{I3})$$

where we have applied the same technique as in Section IV B of separating the negative and positive parts of the P-representation, but applying the step function instead of $\epsilon(\epsilon_0, r^2)$. Since all of the mass of $P_s^{(m,m)}$ concentrates around the origin as $s \rightarrow 0$ (since the decay exponent becomes larger as s decreases), the second term approaches 0 as s does. On the other hand, $\mu_\tau [P_s^{(m,m)}]$ approaches ∞ . Following the methods used in Eq. (F13), we get (for $s < \frac{1}{2}$)

$$\mu_\tau [P_s^{(m,m)}] \leq 2 \left(1 - e^{-\tau^2 \frac{1-2s}{2s(1-s)}} \right) \frac{(1-s)^{m+1}}{s^m(1-2s)}, \quad (\text{I4})$$

so we can write the upper bound

$$\|(\Psi - \Phi)[\mathcal{C}_s(|m\rangle\langle m|)]\| \leq 2 \frac{(1-s)^{m+1}}{s^m(1-2s)} \left(\epsilon_0 + (2 - \epsilon_0) e^{-\tau^2 \frac{1-2s}{2s(1-s)}} \right). \quad (\text{I5})$$

Noting that Eq. (I5) is trivial for large m , we provide the non-trivial bound $\|(\Psi - \Phi)[\mathcal{C}_s(|m\rangle\langle m|)]\| \leq \xi_{\tau,s}^{(m,m)}$, where

$$\xi_{\tau,s}^{(m,m)} = \min \left[2 \frac{(1-s)^{m+1}}{s^m(1-2s)} \left(\epsilon_0 + (2 - \epsilon_0) e^{-\tau^2 \frac{1-2s}{2s(1-s)}} \right), 2 \right]. \quad (\text{I6})$$

Following a similar approach for the off-diagonals, we recall that the P-representation of $\frac{1}{2}\mathcal{C}_s(e^{i\theta}|m\rangle\langle n| + e^{-i\theta}|n\rangle\langle m|)$ is given by Eq. (F2). Proceeding similarly to the on-diagonal case, we must find $\mu_\tau [P_s^{(m,n)}]$. Following Eq. (F9), we get

$$\mu_\tau [P_s^{(m,n)}] \leq \frac{2^{2+\frac{m-n}{2}} (1-s)^{1+\frac{m+n}{2}} (m-n+1)_n}{\pi s^{\frac{m+n}{2}} (1-2s)^{1+\frac{m-n}{2}} \sqrt{m!n!}} \left(\Gamma \left[1 + \frac{m-n}{2} \right] - \Gamma \left[1 + \frac{m-n}{2}, \frac{\tau^2(1-2s)}{2s(1-s)} \right] \right), \quad (\text{I7})$$

where $\Gamma[a, b]$ is the incomplete gamma function. We get the bound $\frac{1}{2} \|(\Psi - \Phi)[\mathcal{C}_s(e^{i\theta}|m\rangle\langle n| + e^{-i\theta}|n\rangle\langle m|)]\| \leq \xi_{\tau,s}^{(m,n)}$, where

$$\xi_{\tau,s}^{(m,n)} = \min \left[\frac{2^{2+\frac{m-n}{2}}(1-s)^{1+\frac{m+n}{2}}(m-n+1)_n}{\pi s^{\frac{m+n}{2}}(1-2s)^{1+\frac{m-n}{2}}} \frac{(m-n+1)_n}{\sqrt{m!n!}} \left(\epsilon_0 \Gamma \left[1 + \frac{m-n}{2} \right] + (2-\epsilon_0) \Gamma \left[1 + \frac{m-n}{2}, \frac{\tau^2(1-2s)}{2s(1-s)} \right] \right), 2 \right]. \quad (18)$$

Finally, putting these various elements together, we get

$$\|(\Psi - \Phi)[|re^{i\phi}\rangle\langle re^{i\phi}|_{\text{coh}}]\| \leq \epsilon(\epsilon_0, r^2) = \min \left[\inf_{0 < s < \frac{1}{2}} \left\{ e^{-r^2} \sum_{m,n=0}^{\infty} \frac{r^{m+n}}{\sqrt{m!n!}} \xi_{\tau,s}^{(m,n)} + 4\sqrt{s(1+2r^2)} \right\}, 2 \right]. \quad (19)$$

From Eqs. (16) and (18), we see that decreasing ϵ_0 (or increasing τ) for fixed s decreases $\xi_{\tau,s}^{(m,n)}$. For sufficiently small ϵ_0 , we can choose s such that Eq. (19) is non-trivial for any r . Eq. (19) is not known to be concave, but we can always make it concave by taking its upper concave hull. Nonetheless, it is not a practically useful bound, as we require ϵ_0 to be extremely small for it to be non-trivial for large r . However, it is sufficient to prove that a concave bounding function $\epsilon(\epsilon_0, r^2)$ can always be constructed, and hence that out-of-distribution generalisation is always possible.

Appendix J: Tightening the bound for SPATs

For low energy SPATs, the negativity is large, so the bound on the distance between the output states, given by Eq. (34), may be loose. To tighten it, we may consider using the same technique as for states with infinite negativity, i.e., we can bound the output distance for the input $\sigma_{s,\text{SPAT}}$, where $\sigma_{s,\text{SPAT}}$ is given by applying the Gaussian additive noise channel \mathcal{C}_s to ρ_{SPAT} . The distance between ρ_{SPAT} and $\sigma_{s,\text{SPAT}}$ is given by Eq. (16). Parametrising with q instead of \bar{n} , we get $\delta_s \leq 2\sqrt{s(3+4q)}$.

Using the P-representation of ρ_{SPAT} from Eq. (31), we find the P-representation of $\sigma_{s,\text{SPAT}}$ is

$$\left(\frac{1}{s\pi} e^{-\frac{1}{s}|\alpha|^2} \right) \star P_{\text{SPAT}}(re^{i\phi}) = \frac{1+q}{\pi(q+s)^3} \left(r^2 - \frac{(q+s)(1-s)}{1+q} \right) e^{-\frac{r^2}{q+s}}. \quad (J1)$$

Integrating separately over the negative ($r^2 < \frac{(q+s)(1-s)}{1+q}$) and positive regions, we find the values of μ_s and $\frac{\nu_s}{\mu_s}$ for $\sigma_{s,\text{SPAT}}$ are

$$\mu_s = 2e^{-\frac{1-s}{1+q}} \frac{1+q}{q+s} - 1, \quad \frac{\nu}{\mu} = 1 + 2q + s - \frac{2(1-s)^2}{2 + 2q - e^{-\frac{1-s}{1+q}}(q+s)} < 1 + 2q + s. \quad (J2)$$

We can then write the bound

$$\|(\Psi - \Phi)[\rho_{\text{SPAT}}]\| \leq \left(2e^{-\frac{1-s}{1+q}} \frac{1+q}{q+s} - 1 \right) \epsilon \left(\epsilon_0, 1 + 2q + s - \frac{2(1-s)^2}{2 + 2q - e^{-\frac{1-s}{1+q}}(q+s)} \right) + 4\sqrt{s(3+4q)}, \quad (J3)$$

which reduces to Eq. (34) in the limit of $s \rightarrow 0$. Since the argument to concave function ϵ is approximately linear in s , a small change in s may not increase $\epsilon(\epsilon_0, \frac{\nu}{\mu})$ by much. The δ_s term is also sublinear in s . On the other hand, for small q , a small change in s can result in a significant change in the multiplicative factor μ_s . Hence, we may obtain tighter bounds by choosing $s > 0$.

Appendix K: Application to squeezed vacuums

Using Eqs. (F15), (F16), and (38), we can calculate $\mu_{s,M}$ for a (one-mode) squeezed vacuum, by calculating the contributions from each element of ρ_{sq} . For any off-diagonal element with $p > q$,

$$|\langle 2p|\rho|2q\rangle|_{\mu_{s,2p,2q}} = \frac{4\sqrt{1-\lambda^2}(1-s)}{\pi(1-2s)^{p-q+1}} \frac{(1-s)^{p+q}\lambda^{p+q}}{s^{p+q}} \frac{(1+2p-2q)_{2q}(p-q)!}{2^{2q}p!q!} \quad (K1)$$

where we have separated out terms based on their dependence on p and q . For on-diagonal elements,

$$|\langle 2p|\rho|2p\rangle|_{\mu_{s,2p,2p}} = \frac{2\sqrt{1-\lambda^2}(1-s)}{(1-2s)} \frac{(1-s)^{2p}\lambda^{2p}}{s^{2p}} \frac{(2p)!}{2^{2p}(p!)^2}. \quad (K2)$$

Note that iff $\frac{(1-s)\lambda}{s} < 1$, the sum $\sum_q |\langle 2(p_0+q)|\rho|2q\rangle|_{\mu_{s,2(p_0+q),2q}}$ for q ranging from 0 to ∞ is convergent. This is as expected, since $\frac{(1-s)\lambda}{s} < 1$ is precisely the condition for the negativity of a squeezed vacuum to be finite (in fact, zero). However, we want to be able to take s to 0 as $\epsilon_0 \rightarrow 0$, so we are interested in the divergent region. Instead, we set $x = \frac{(1-2s)(1-s)\lambda}{s}$, so that

$$\begin{aligned} \sum_{q=0}^{p-1} |\langle 2p|\rho|2q\rangle|_{\mu_{s,2p,2q}} &= \frac{4\sqrt{1-\lambda^2}}{\pi} \frac{\lambda^p(1-s)^{p+1}}{s^p(1-2s)^{p+1}} \sum_{q=0}^{p-1} \frac{x^q(1+2p-2q)_{2q}(p-q)!}{2^{2q}p!q!} \\ &= \frac{4\sqrt{1-\lambda^2}}{\pi} \frac{\lambda^p(1-s)^{p+1}}{s^p(1-2s)^{p+1}} \left((1+x)^{p-\frac{1}{2}} - \frac{x^p {}_2F_1\left(\frac{1}{2}, 1, 1+p, -x\right)(2p)!}{2^{2p}(p!)^2} \right), \end{aligned} \quad (\text{K3})$$

where ${}_2F_1$ is the hypergeometric function. Multiplying by two to account for $p < q$ and adding the on-diagonal contribution,

$$\begin{aligned} |\langle 2p|\rho|2p\rangle|_{\mu_{s,2p,2p}} + 2 \sum_{q=0}^{p-1} |\langle 2p|\rho|2q\rangle|_{\mu_{s,2p,2q}} &= \frac{8\sqrt{1-\lambda^2}}{\pi} \frac{\lambda^p(1-s)^{p+1}}{s^p(1-2s)^{p+1}} \left((1+x)^{p-\frac{1}{2}} \right. \\ &\quad \left. + \frac{x^p(2p)!}{2^{2p}(p!)^2} \left(\frac{\pi}{4} - {}_2F_1\left(\frac{1}{2}, 1, 1+p, -x\right) \right) \right). \end{aligned} \quad (\text{K4})$$

Applying a Pfaff transformation to the hypergeometric function so that its final argument is $\frac{x}{1+x}$ and then writing it in power series form, we can easily verify that it is always positive. Hence, we can upper bound this expression with

$$\begin{aligned} |\langle 2p|\rho|2p\rangle|_{\mu_{s,2p,2p}} + 2 \sum_{q=0}^{p-1} |\langle 2p|\rho|2q\rangle|_{\mu_{s,2p,2q}} &\leq \frac{2(1-s)\sqrt{1-\lambda^2}}{(1-2s)} \left(\frac{4}{\pi\sqrt{(1+x)}} \left(\frac{\lambda(1-s)(1+x)}{s(1-2s)} \right)^p \right. \\ &\quad \left. + \frac{(2p)!}{2^{2p}(p!)^2} \left(\frac{\lambda(1-s)x}{s(1-2s)} \right)^p \right). \end{aligned} \quad (\text{K5})$$

The first term is a geometric sequence in p , so is simple to sum. For the second term, $\frac{(2p)!}{2^{2p}(p!)^2} \leq 1$ (this can be simply verified by taking the ratio between this expression for p and $p+1$ and thus seeing it is a decreasing function of p). Hence, we can upper bound the second term by replacing $\frac{(2p)!}{2^{2p}(p!)^2}$ with its maximum value of 1. Then, both terms are geometric sequences, so we can recover Eq. (39) by summing over p (note that the maximum value of p is $\frac{M+1}{2}$, not $M-1$).